ELSEVIER

Tectonophysics 345 (2002) 299–327

TECTONOPHYSICS

www.elsevier.com/locate/tecto

Structure of the Mérida Andes, Venezuela: relations with the South America–Caribbean geodynamic interaction

Felipe E. Audemard [a], Franck A. Audemard [b,*]

[a] *PDVSA Exploración y Producción, Caracas, Venezuela*
[b] *Earth Sciences Department, Venezuelan Foundation for Seismological Research, FUNVISIS, Apartado Postal 76880, Caracas 1070-A, Venezuela*

Received 28 March 2000; received in revised form 5 April 2001; accepted 11 April 2001

Abstract

For over 50 years, several models based on diverse geologic concepts and variable quality of data have been proposed to explain the major structure and history of the Mérida Andes (MA), in western Venezuela. Lately, this chain growth and associated flexural basins deepening have been related to incipient type-A subductions of either polarity, accounting for the across-chain asymmetry. However, these recent models have not well integrated the present tectonically active setting driven by neighboring major plate interactions. At present, this chain exhibits ongoing strain partitioning where cumulative right-lateral slip along chain axis is as much as half of, or about the same, as the transverse shortening since late Miocene, thus implying that the NNE-directed Maracaibo block extrusion with respect to the South America (SA) plate is not a secondary feature. Consequently, this paper discusses some limitations exhibited by the SE-directed continental subduction models—Maracaibo crust underthrusting the Mérida Andes—in the light of available geological and geophysical data. Besides, it is herein proposed that the Mérida Andes structuration is related to a NW-directed, gently dipping, incipient type-A subduction, where chain growth and evolution are similar to those of a sedimentary accretionary wedge (i.e., Barbados), but at crustal scale and with ongoing strain partitioning. This continental subduction is the SE portion of a major orogenic float that also comprises the Perijá range and the Santa Marta block.

Keywords: triangular zones; strain partitioning; type-A subduction; crustal models; Mérida Andes; Venezuela

1. Introduction

The Mérida Andes (MA) is in the northeastward topographic prolongation of the Eastern Cordillera (EC) of the Colombian Andes. The latter belongs to the main Andes chain that extends all along the Pacific coast of South America (SA). However, the MA and EC do not keep direct genetic relationship between them (Fig. 1) since the present NE–SW trending Venezuelan (or Mérida) Andes are not related to direct interactions between the SA craton and either arc terrains or oceanic domains, as the rest of the SA Andes does. Besides, both chains are separated by the southern termination of the left-lateral strike-slip (LLSS) Santa Marta–Bucaramanga fault (SMBF) and the NW–SE trending Santander Massif (SM). As a matter of fact, the MA formation has always

* Corresponding author. Tel.: +58-212-2577672; fax: +58-212-2579977.
E-mail address: faudem@internet.ve (F.A. Audemard).

0040-1951/02/$ - see front matter
PII: S0040-1951(01)00218-9

been linked to indirect plate interactions. For instance, an older less-prominent MA chain formed in the Miocene (Fig. 9.11 of Audemard, 1993; Audemard, 1998), probably related to the early stages of collision of the Panamá Arc (PA) against western SA. This first pulse in the MA was probably coeval with uplift in the EC reported by Taboada et al. (2000). This first orogenic pulse drove deposition of molassic deposits along the southern and northern MA flanks named as Parángula and Isnotú formations, respectively. On the other hand, the present chain build-up results from Pliocene–Quaternary transpression due to oblique convergence between two independent continental blocks. This Plio–Quaternary compression is superposed to the first Miocene compressional phase. Therefore, Jurassic (half-) grabens have been inverted by these two consecutive compressional phases, thus exposing Precambrian and Paleozoic rocks of the SA continental crust.

2. Previous crustal models

Several models have been proposed to explain the major structure of the MA during the last 50 years. They may be essentially gathered in two major conceptual models. On one hand, some models have conceived the MA as an essentially symmetric chain to a major axial strike-slip fault, with both sides bounded by reverse faults—responsible for chain vertical growth—(González de Juana, 1952; Rod, 1956b). Consequently, the MA would resemble a positive flower structure. This model was also shared by Dallmus (1957, in Rod et al., 1958), at least for the upper crustal level; later on, Stephan (1985) still maintained this interpretation. On the other hand, several other models incorporated more recently the asymmetry of the MA revealed by the gravimetric survey of Hospers and Van Wijnen (1959), though the chain asymmetry was first evoked by De Cizancourt (1933) and later by Bucher (1952)—before the survey was performed—but their models did not display the crustal-scale structure. Among the asymmetric models, there are two trends depending on the major underthrusting vergence. For instance, Audemard (1991) indicates that major structuration of the MA results from a NW-vergent crustal-scale wedging rooted on top of a crustal NW-gently dipping detachment. Instead, Jácome et al. (1995) propose an "orogenic float" model. On the contrary, Kellogg and Bonini (1982), De Toni and Kellogg (1993), Sánchez et al. (1994) and Colletta et al. (1997) favor the SE polarity models. Additional to the conceptual application of very incipient type-A subduction or crustal delamination to the MA, most recent papers on the chain and its related basins (Kellogg and Bonini, 1982; Audemard, 1991; De Toni and Kellogg, 1993; Sánchez et al., 1994; Castrillo, 1997; Colletta et al., 1997; Funvisis, 1997; Duerto, 1998; Duerto et al., 1998) also incorporate new modern concepts at crustal or lithospheric scale: flexural basins, blind thrusts, intracutaneous wedges and triangular zones.

It is worth mentioning that the actual chain asymmetry does not completely discard the early positive flower structure models if it is considered that transpression could invert an initially asymmetric Jurassic rift geometry. This original rift asymmetry has been incorporated in the model proposed by Colletta et al. (1997), where the NW bounding fault exhibits slightly steeper dip than its SE counterpart (Plate 1 of Colletta et al., 1997).

At both crustal and regional scale, all these models rely on partial geological and/or geophysical data, thus only having local significance. Besides, most of them have much underestimated the role of regional active tectonics that is controlled by the present plate interaction puzzle. However, a big jump forward in the understanding of the very few first kilometer-thick subsurface structure of both foothills has been achieved due to both amount of oil-prospection geophysical surveys carried out in the last two decades and increasing progress in geophysical data acquisition.

3. Present geodynamic setting

Since the MA orogeny should not be attributed to convergence at a conventional type-B subduction zone, this chain has to be related with the complex interaction among the Caribbean, South America and Nazca plates. Whereas northern Venezuela essentially lies in the rather simple interaction zone between the Caribbean and South America plates, western Venezuela shows a more complex geodynamic setting (Audemard, 2000). A wide consensus establishes that

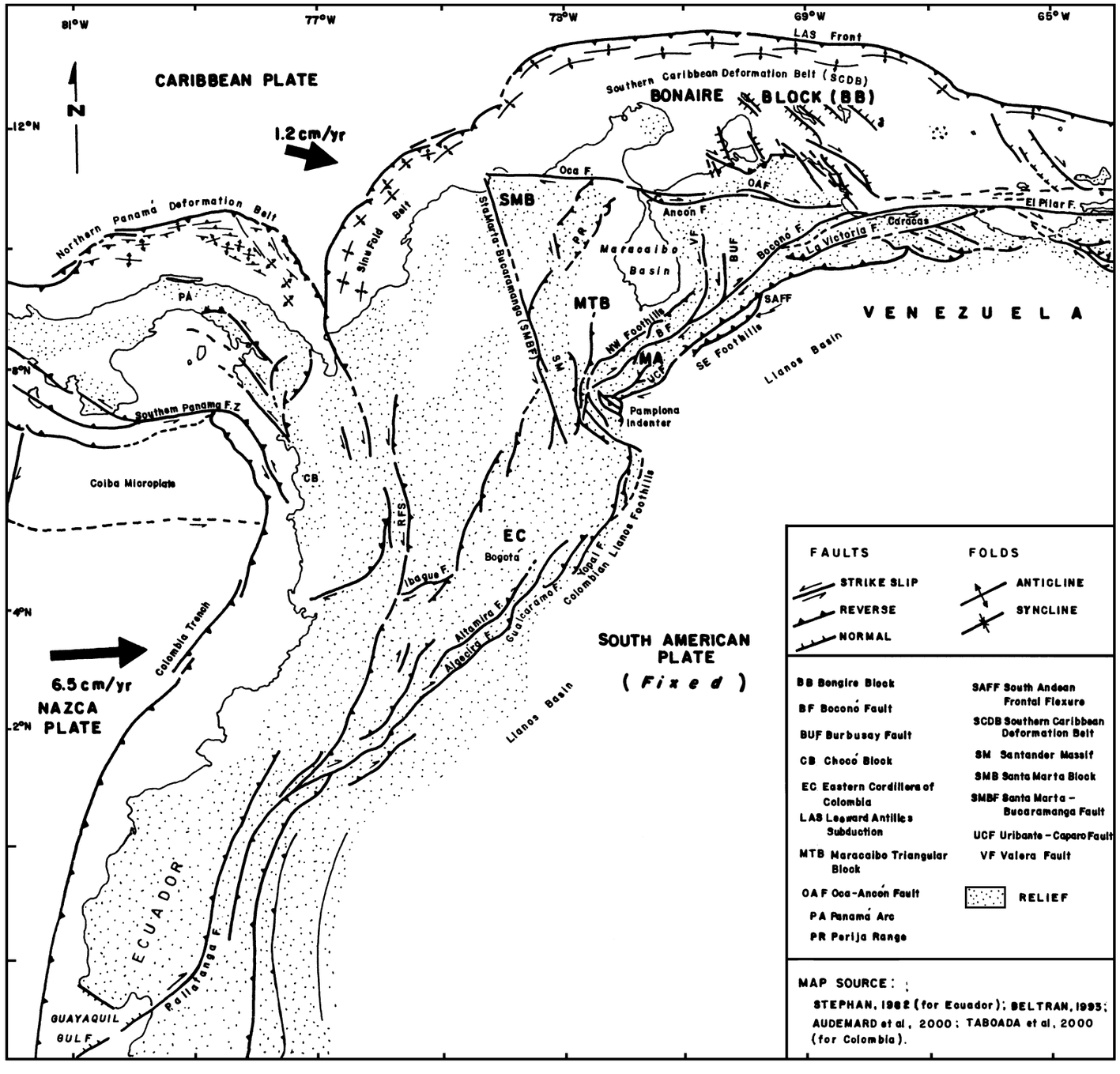

Fig. 1. The Mérida Andes (MA) with respect to the geodynamic setting of the northern Andes, from Ecuador to Venezuela. Abbreviations are kept unchanged for all figures and text. Sources: Stephan (1982), Beltrán (1993), Audemard et al. (2000), Taboada et al. (2000).

the Caribbean plate moves roughly eastward relatively to South America (e.g., Bell, 1972; Malfait and Dinkelman, 1972; Jordan, 1975; Pindell and Dewey, 1982; Sykes et al., 1982; Wadge and Burke, 1983; Freymueller et al., 1993; Kellogg and Vega, 1995; among others), but this active plate boundary is not of the simple dextral type (Soulas, 1986; Beltrán, 1994) since it is an over 100-km-wide active transpressional zone (Audemard, 1993, 1998; Singer and Audemard, 1997). Important reliefs (the Coast and Interior ranges along the northern coast) are associated to this east–west trending northern boundary. This boundary extends southwestward into the MA, where strain is partitioned between the right-lateral strike-slip (RLSS) Boconó fault (BF) roughly running along the axis of the chain and thrust faults bounding the chain on both flanks.

As a matter of fact, the plate boundary in western Venezuela is up to 600 km wide and comprises a set of discrete tectonic blocks, independently moving among the surrounding larger plates (Caribbean, South America and Nazca; Figs. 1 and 2), among which the Maracaibo triangular block (MTB) stands out (Audemard, 2000). This independent block is bounded by the LLSS Santa Marta–Bucaramanga fault (SMBF) in Colombia and RLSS Boconó fault in Venezuela and separated on the north from the Bonaire block (BB) by the RLSS Oca-Ancón fault (Fig. 1). Besides, both Maracaibo and Bonaire blocks are roughly being extruded to NNE with respect to SA and are overriding the Caribbean plate north of the Leeward Antilles islands (Figs. 1 and 2), where a young south-dipping, amagmatic, flat oceanic sub-

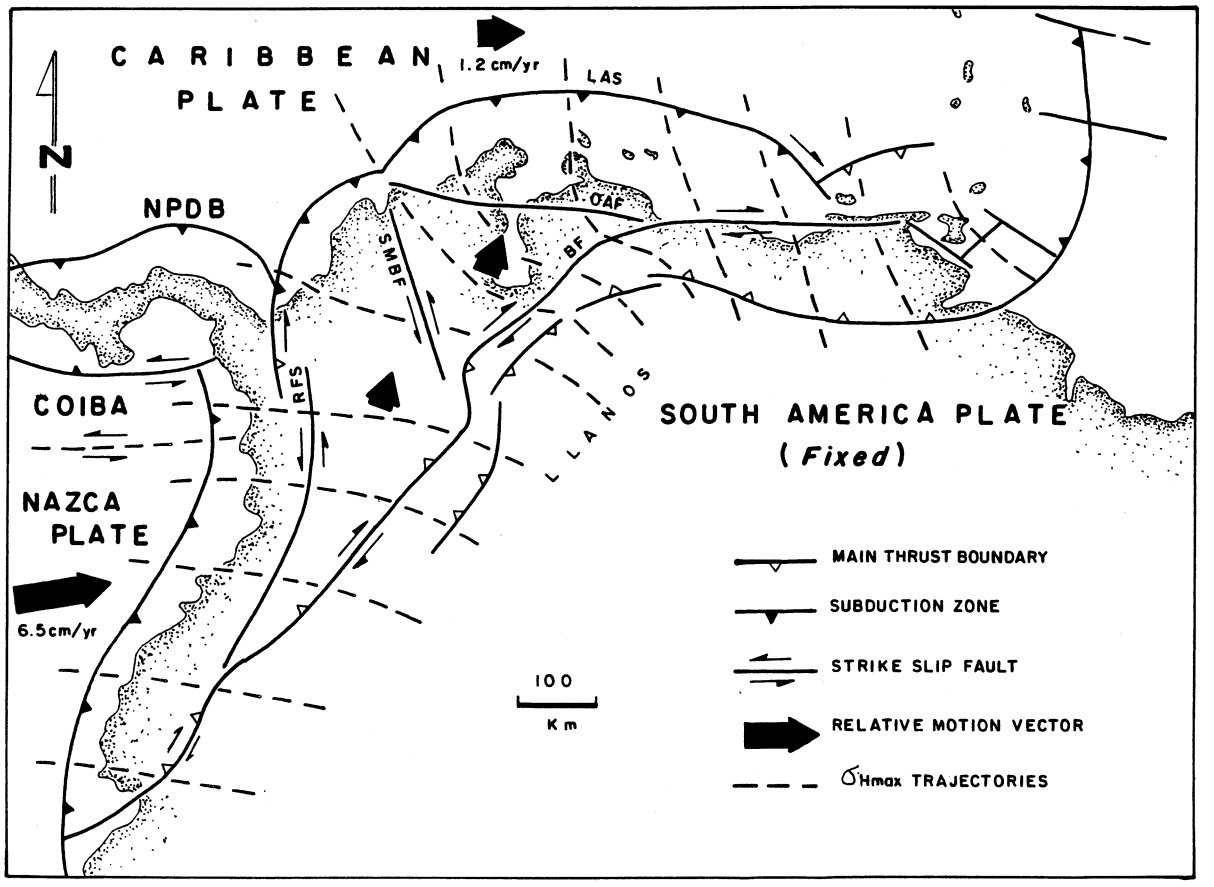

Fig. 2. Schematic geodynamic setting of northwestern South America, showing the maximum horizontal stress trajectories and relative motion vectors with respect to South America (active tectonics and trajectories modified from Stephan, 1982; Beltrán and Giraldo, 1989, respectively).

duction has been forming in the last 5 Ma (Audemard, 2000). Extrusion of these blocks is related to the collision of the Panamá Arc (PA) against the Pacific side of northern South America and its later suturing (Audemard, 1993, 1998). Recent results from GPS plate motion studies (Freymueller et al., 1993; Kellogg and Vega, 1995; Kaniuth et al., 1999) confirm the northeastward escape of both blocks relative to all surrounding blocks. This adds amount of convergence along the southern Caribbean deformation belt (SCDB) north of the Netherlands Leeward Antilles to the relative convergence of both Americas. The Leeward Antilles Subduction (LAS)—responsible for the SCDB—is a rather young feature and should not be confused with the Caribbean Plate subduction (CPS) that led to the collision of the PA against western SA along the Chocó block (CB) and San Jacinto terranes (Fig. 1). In fact, the original CPS (hereafter this solely refers to the one prior to the PA–SA collision) used to trend roughly north–south along the western coast of SA and to extend as far north as NW of the town of Santa Marta. This major plate boundary is a rather straight feature as old as Cretaceous in certain models, which remained essentially unchanged during most of the Paleogene and early Neogene (Pindell and Dewey, 1982; Wadge and Burke, 1983; Beck, 1985; Pindell et al., 1988; Ross and Scotese, 1988; Stephan et al., 1990; Taboada et al., 2000). It is worth mentioning that in some previous models where the CPS is prolonged around the northwestern corner of SA, some authors have been cautious about its northward extension beyond northern Colombia since the east–west trending, south-dipping oceanic subduction segment under northern Venezuela (equivalent to the present LAS) is shown as a dashed feature (e.g., Malfait and Dinkelman, 1972; Taboada et al., 2000). However, there seems to be some inheritance of the latter LAS from the former CPS since the younger LAS progressed northward and bent eastward progressively from the old CPS around the northwestern corner of SA. Therefore, this convex-to-the-north arcuate LAS actually roughly trends east–west, almost perfectly normal to the one sinking under western SA. The model proposed by Taboada et al. (2000) shows that those two subduction slabs—though both composed of abnormally thick Caribbean oceanic lithosphere—are essentially two discrete entities that have reached different depths into the astenosphere. This could suggest that both subduction slabs are of different age, the LAS being much younger. Duque-Caro (1978) proposes an LAS activation age of about 10 Ma ago, whereas Audemard (1993, 1998) suggests 5–3 Ma, directly related to the expulsion of the MTB, induced by the suturing of the PA against western SA. The subduction along the LAS is incipient. This is supported by the total 400–450 km length of flat (16°S) slab subducted under northwestern SA (Kellogg and Bonini, 1982; Van der Hilst and Mann, 1993) that allows to cut across the lithosphere and just get into the astenosphere. Besides, the present intermediate seismicity only reaching up to 200 km in depth (e.g., Dewey, 1972; Kellogg and Bonini, 1982; Malavé and Suárez, 1995) is an additional evidence to the incipient evolutionary stage of this slab.

4. Strain partitioning

The previously described geodynamic setting is responsible for ongoing strain partitioning along the MA where the foothills and the mountain belt have been shortened transversely in a NW–SE direction, whereas the Boconó fault—roughly located in the core and along the MA axis—accommodates dextral slip. This strain on the MTB and south of the Oca-Ancón fault (OAF) is related to the present stress field that progressively turns counterclockwise (Beltrán and Giraldo, 1989) from a NNW–SSE orientation along northern Venezuela to become more east–west oriented in the southern MA (Fig. 2; Audemard et al., 1999b). This spatially varying stress field allows left- and right-lateral slip along the north–south striking (e.g., Valera and Burbusay) and NE–SW striking (e.g., Boconó, Caparo, Queniquéa, San Simón) faults, respectively. This regional stress field in western Venezuela results from the vectorial addition of the two major neighboring interplate maximum horizontal stresses (σ_H): east–west trending stress across the Nazca–South America type-B subduction along the Pacific coast of Colombia and NNW–SSE oriented one across the Caribbean southern boundary (Audemard, 2000). Therefore, the MTB is simultaneously being shortened in NW–SE direction (expressed by the vertical growth of the Santa Marta block and

Perijá and Mérida ranges) and roughly extruded north to NNE (Audemard, 1993, 1998, 2000).

Within the transpressional Caribbean–South America boundary zone, a large portion of the dextral motion seems to take place along the major RLSS Boconó–San Sebastián–El Pilar–Los Bajos fault system (Fig. 1; Molnar and Sykes, 1969; Minster and Jordan, 1978; Pérez and Aggarwal, 1981; Stephan, 1982; Schubert, 1984; Soulas, 1986; Beltrán and Giraldo, 1989; Singer and Audemard, 1997). This major boundary slips at about 1 cm/year (Soulas, 1986; Freymueller et al., 1993), whereas secondary faults at least slip one order of magnitude less faster; as a matter of fact, most of them exhibit slip rates under 0.5 mm/year, except for Oca-Ancón (2 mm/year), Burbusay (≤ 3 mm/year), Valera and La Victoria (≤ 1 mm/year) faults.

5. Chain segmentation along strike

Based on major structures shaping the chain, the MA may be subdivided into two different portions (Fig. 3).

(a) A northern portion that extends north of the Valera–Boconó faults convergence (transverse boundary slightly north of Barinas), which is characterized by: (1) the absence of a conspicuous NW-vergent thrust front along the northwestern boundary, (2) a Boconó fault in axial position and (3) the existence of a SE-vergent thrust front along the Llanos basin.

(b) A southern portion characterized by: (1) a well developed NW-vergent thrust front, responsible for development of triangular zones within the Late Cretaceous–Tertiary sedimentary sequence of the Maracaibo basin and deepening of that basin by lithostatic forces (flexural basin), (2) a Boconó fault shifted northward with respect to the chain axis and (3) lack of or poorly developed SE-vergent southern foothills front. This major structuration results from the Pamplona indenter, which verges westward, as attested by the left-lateral slip of the Bramón–Chucarima–Pamplona fault system on the northeastern side of the Santander Massif, thrusting along the Chinacotá fault and the northward displacement of the RLSS Boconó fault trace with respect to the Colombian Llanos Foothills Fault system (CLFFS) along the eastern edge of the EC (Fig. 1).

6. The Bócono fault

The NE–SW trending RLSS Boconó fault runs slightly oblique to the MA chain axis and its northeastern tip bounds the Caribbean Coast range of northern Venezuela on the west, thus extending for about 500 km between the Tachira depression at the border between Colombia and Venezuela, and Morón on the Caribbean coast of Venezuela. At its north end at the coast, the Boconó fault exhibits a 45° clockwise bend that allows prolongation into the east–west striking San Sebastián–El Pilar system (Fig. 1). To the south, the Boconó fault connects with the CLFFS (Guaicaramo fault) through the Bramón–Chucarima–Pamplona fault system after undergoing two opposite right-angle bends (Fig. 1), a structure known as the Pamplona indenter (Boinet, 1985). The CLFFS seems to extend as far south as the Jambeli graben (Guayaquil, gulf, Ecuador), thus splitting the northwestern corner of South America from the rest of the continent (Stephan, 1982; Figs. 1 and 2).

The Boconó fault has been identified, mapped and characterized rather easily by the large number of along-strike geomorphic features, among which: continuous series of aligned 1–5-km-wide valleys and linear depressions, passes, saddles, trenches, sag ponds, scarps and sharp ridges (e.g., Rod, 1956b; Schubert, 1980a,b, 1982; Giraldo, 1985; Soulas, 1985; Soulas et al., 1986; Soulas and Singer, 1987; Casas, 1991; Ferrer, 1991; Singer and Beltrán, 1996; Audemard et al., 1999a). Right-lateral offsets of Quaternary features such as mountainous ridges, drainages, alluvial deposits and shutter ridges, range from 60 to 1000 m depending on their age. These offsets yield a Quaternary slip rate between 3 and 14 mm/year (for a complete review, see Schubert, 1982). Recent studies in the Mucubají area (Schubert, 1980a; Soulas, 1985; Soulas et al., 1986) obtained an average slip rate of about 5–9 mm/year, based on 60–100 m of dextral offset (measurement dispersion depends on authors) of the Los Zerpa moraines, which are radiocarbon-dated at a minimum of about 13-ka old. These rates are essentially consistent with those predicted by plate motion models of about 1 cm/year, assuming that the Boconó fault is part of the main boundary between the MTB and South America plate (e.g., Molnar and Sykes, 1969; Minster and Jordan, 1978; Soulas, 1986; Freymueller et al., 1993).

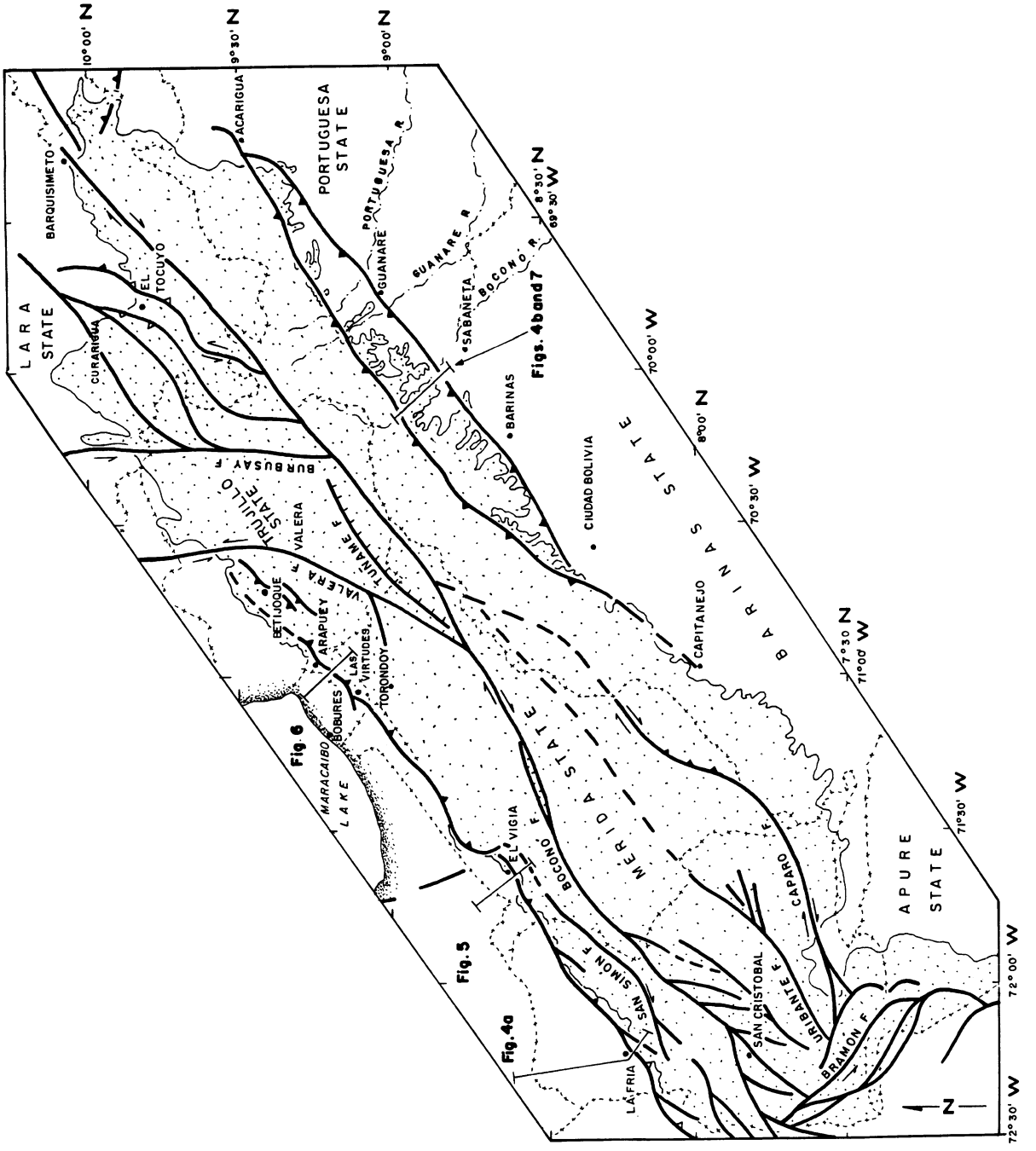
10°00' N
9°30' N
9°00' N
8°30' N
69°30' W
70°00' W
70°30' W
71°00' W
71°30' W
72°00' W
72°30' W
LARA STATE
PORTUGUESA STATE
BARINAS STATE
APURE STATE
TRUJILLO STATE
MERIDA STATE
BARQUISIMETO
CURARIGUA
EL TOCUYO
ACARIGUA
PORTUGUESA R.
GUANARE
GUANARE R.
SABANETA
BOCONO R.
BARINAS
CIUDAD BOLIVIA
CAPITANEJO
BURBUSAY F.
VALERA
TUNAME F.
VALERA F.
BETIJOQUE
ARAPUEY
LAS VIRTUDES
TORONDOY
BOBURES
MARACAIBO LAKE
EL VIGIA
BOCONO F.
SIMÓN F.
SAN
LA FRIA
SAN CRISTOBAL
URIBANTE F.
CAPARO
BRAMÓN F.
Z
Fig. 6
Fig. 5
Fig. 4a
Figs. 4b and 7

The Boconó fault slip rate decreases towards both ends. South of where the fault is the fastest (near Mucubají), average slip rate decreases to 5.2 ± 0.9 mm/year between Mérida and San Cristobal (Audemard, 1997a) and as little as a 1 mm/year at the Venezuela–Colombia border (Singer and Beltrán, 1996). The apparent lower slip rate may be the result of displacement transfer into the Pamplona indenter convergence, slip distribution along at least three active strands of the Boconó fault system in the southern Andes and slip transfer to other subparallel active faults, such as the Queniquéa, San José, Uribante-Caparo and Seboruco faults, among others (Fig. 3). The rate reduction is then expressed in a longer recurrence interval between equivalent earthquakes on the Boconó fault near Cordero (Audemard, 1997a). Similarly, subparallel and branching faulting along the northernmost portion of the Boconó fault may explain the slip rate drop (1.5–3 mm/year) reported by Casas (1991), along the Yaracuy Valley.

7. The Mérida Andes foothills

As mentioned earlier, strain partitioning is taking place throughout the MA. Thus, significant thrusting occurs subparallel to the RLSS Boconó fault on both sides of the MA, accommodating a rather large amount of shortening across the chain (Gonźalez de Juana, 1952; Rod, 1956b; Hospers and Van Wijnen, 1959; Schubert, 1968; Kellogg and Bonini, 1982; Henneberg, 1983; Soulas, 1985; Audemard, 1991; De Toni and Kellogg, 1993; Jácome, 1994; Sánchez et al., 1994; Colletta et al., 1996, 1997; Audemard, 1997b; Duerto et al., 1998).

A good knowledge of the subsurface structure of both foothills has been acquired from a large set of geophysical surveys in the Maracaibo and Barinas–Apure basins but most of the deep structure of the chain remains unknown. Only the Moho depth has been estimated in certain areas (29 km for the Maracaibo crust by Padrón and Izarra, 1996) and the general mass distribution has been derived from gravimetric profiles and surveys (e.g., Hospers and Van Wijnen, 1959; Bonini et al., 1977).

The seismic surveys confirmed the dominant NW vergence of the MA because a rather deep conventional flexural basin developed on the northwest (the Maracaibo basin; Fig. 4a). A much shallower flexural basin formed to the southeast, although SE-thrusting has been identified within the Tertiary sedimentary sequence, mainly northeast of Barinas (Fig. 4b).

7.1. The northwestern foothills

Although the northwestern Andean thrust front of the MA exhibits a well developed NW vergence, this foothills may be subdivided into two distinct provinces (Audemard, 1991). A southwestern segment southwest of El Vigia is associated with a major passive roof backthrust decoupled from the Upper Cretaceous Colón Formation, where the overlying Tertiary sedimentary sequence dips NW at high angle in a belt of some 10 km in width along the foothills. The upper part of this sequence, comprising the Late Miocene Isnotú Formation and the Plio–Pleistocene Betijoque Formation, displays a chainward-pinching out (upward convergent) wedge, where onlaps of seismic reflectors evidence several progressive unconformities (Fig. 5). In fact, this wedge dates the growth and uplift of this flank of the MA and the syntectonic sedimentary package is essentially Late Miocene to Pleistocene in age. Under this wedge and above the deepest decollement in the Colón shales, two other decollement levels are interpreted by Audemard (1991) and De Toni and Kellogg (1993; Fig. 4a) within the thin Eocene–Oligocene sequences and in between the Lower and Middle Miocene markers, respectively. The SE-backthrusted sequence soles in the Colón Formation and is decoupled by a NW-vergent four-basement-thrust-sheet stack that acts like an intracutaneous wedge (triangular zone; Fig. 5).

The northeastern segment is defined by a major NW verging thrust sheet (Las Virtudes; after Fig. 57 of Audemard, 1991), which acts as a shallow intracutaneous wedge and partly overrides the Tertiary section (Fig. 6). The Upper Miocene–Pleistocene molasse fed by the continuous erosion of the rising MA reaches its maximum thickness of about 8 km near Torondoy (refer to Fig. 3 for location). At the

Fig. 3. Major neotectonic features along the Mérida Andes. Notice their variation along strike (refer to Section 5 for more details). Relative location of figures imaging seismic profiles is also shown. Same legend as Fig. 1.

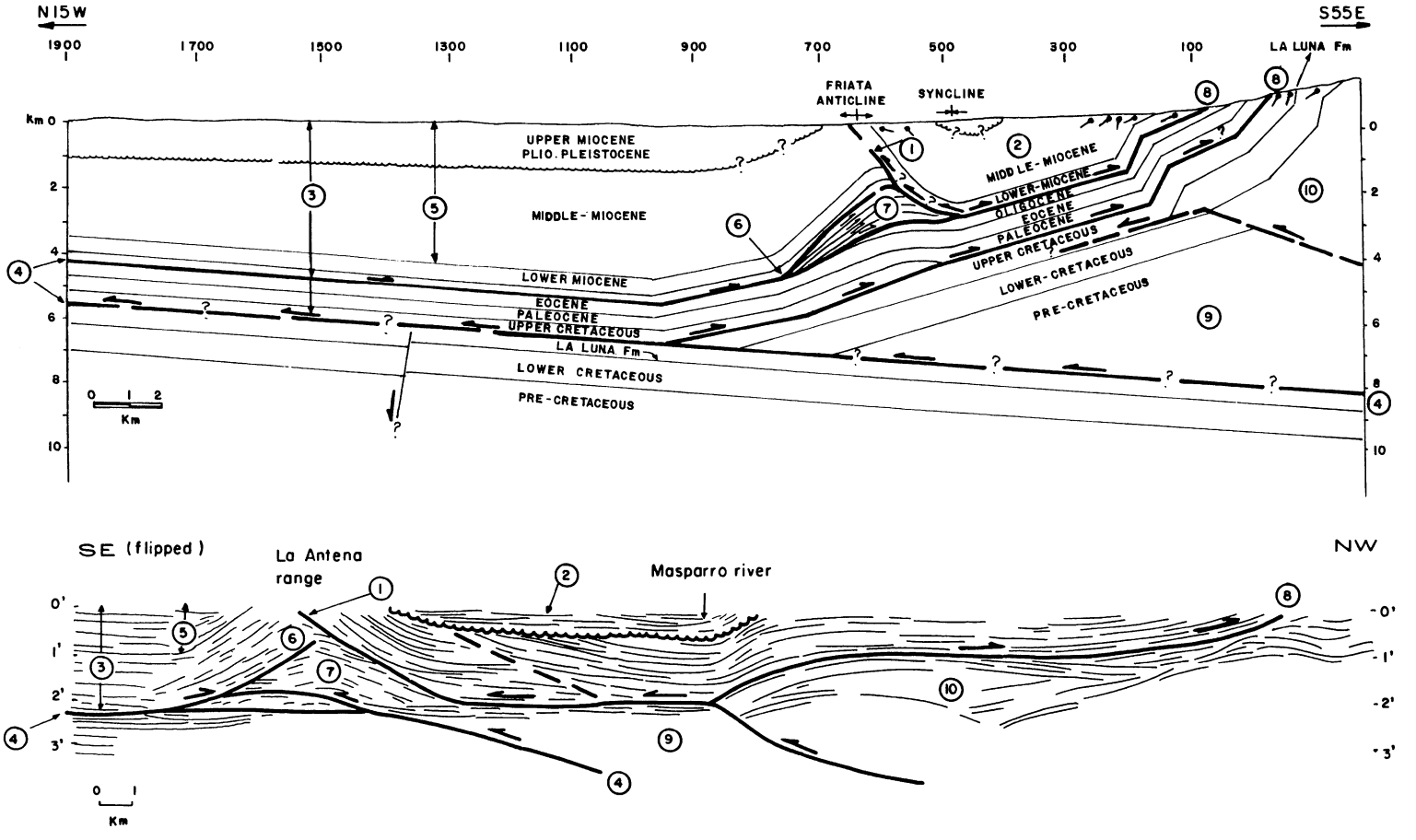

Fig. 4. Many similarities regarding structural styles may be observed between both Mérida Andes (MA) foothills (comparison made easy by labelling; refer to text for further details): (a) structural interpretation across the western foothills at La Fria (after De Toni and Kellogg, 1993; refer to Fig. 3 for location) and (b) line drawing across Las Garzas–Fila La Antena or Peña Larga-anticline in the eastern foothills (after Funvisis, 1997; Audemard, 1999; compare to SA3 line of Fig. 7).

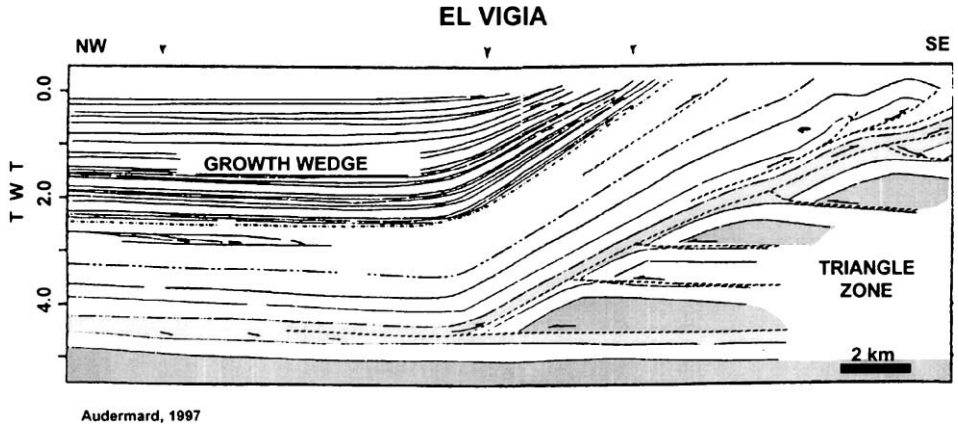

Fig. 5. NW–SE oriented structural interpretation across the northwestern Mérida Andes foothills at El Vigía, showing the well preserved basement-involved intracutaneous wedge and the synorogenic up-dip convergent growth wedge of Late Miocene–Quaternary age (after Audemard, 1997b).

Avispa massif, the Las Virtudes overthrust brings Precambrian and Paleozoic metamorphic rocks, Andean basement, in contact with Tertiary rocks at the mountain front. The thrust is capped by a synorogenic sedimentary wedge containing unconsolidated Plio–Pleistocene sediments of the Betijoque Formation that exhibit the same up-dip convergence wedge as in the southwestern segment (Fig. 6; Audemard, 1991; Castrillo, 1997). This wedge constrains the emplacement age of the shallow sheet as Late Pliocene but an underlying deactivated triangular zone also dates, as for the southern portion, the orogenic onset at the Late Miocene (Audemard, 1991).

Along the northwestern foothills, the northeastern portion of the front shows a more advanced stage than to the southwest—implying more shortening—where the large basement-thrust-stacked intracutaneous wedge (still active in the southern portion) is being destroyed by a shallower basement-involved thrust (Audemard, 1991). This also indicates the existence of out-of-sequence thrusting in the northeastern segment of these foothills.

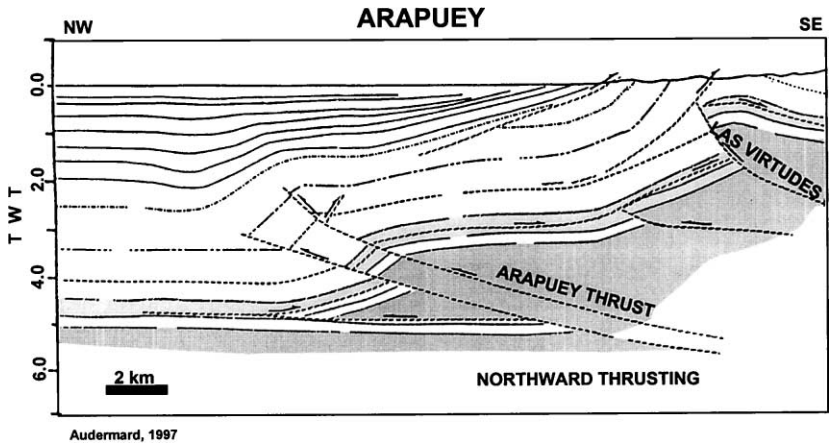

Fig. 6. Schematic NW–SE profile across the Avispa massif and Las Virtudes thrust, in the northwestern Mérida Andes foothills, showing a shallow intracutaneous wedge and the still active synorogenic up-dip convergent growth wedge essentially comprising the Late Pliocene–Quaternary Betijoque Formation. Also notice the underlying fossil triangular zone (after Audemard, 1991, 1997b).

7.2. The southeastern foothills

There is no general agreement regarding the thrust vergence along the southeastern foothills, probably due to masking by triangular zones and intracutaneous wedges, combined with important along-strike variations. For instance, Audemard (1991) proposes that the segment southwest of Barinas displays a predominant NW vergence (e.g., Fig. 2 of Audemard, 1997b) but some authors (i.e., Colletta et al., 1996, 1997) believe that this vergence only occurs at shallow crustal levels, thus being a conjugate imbricated thrust system (backthrust) to a deeper SE vergent thrust. For other authors (Rod, 1960; Stephan, 1982; Castrillo, 1997; Duerto et al., 1998), this foothills vergence is SE directed. Several authors (Giegengack, 1984; Jácome, 1994; Sánchez et al., 1994) even propose dual vergence.

The eastern foothills may show different geometries along strike, the dividing line being somewhere between Capitanejo and Barinas (refer to Fig. 3 for location). The southwestern portion of the southeastern foothills shows a dominant NW vergence with secondary conjugate backthrusting, which is related to the Pamplona indenter. The Pamplona indenter is responsible for convexly bending the southwestern portion of the MA and simultaneously pushing the Boconó fault trace off its axial position. Conversely, the northeastern portion of this foothills exhibits a SE vergence, at least in the upper crustal levels (Funvisis, 1997; Duerto et al., 1998; Audemard, 1999). This thrusting even deforms the Plio–Quaternary molasses (Audemard, 1991, 1999; Funvisis, 1997), as evidenced by a conspicuous flexural scarp that defines the boundary between the foothills unit and the Llanos plains. This NE–SW-trending, SE-facing flexural scarp—known as the South-Andean Frontal flexure (SAFF)—extends for over 200 km between the cities of Barinas and Acarigua. It reaches a maximum height of 300 m above the low topography of the Llanos plains (Audemard, 1999). Lateral continuity of this scarp is interrupted by large drainages such as the Boconó and Guanare rivers. Those river gaps coincide with the lateral terminations of active individual ramps, as suggested by the extent of the exposed Paleogene rocks within the foothills unit (refer to the geologic map of Venezuela by Bellizzia et al., 1976). This has been confirmed by a 3-D seismic survey across the Venezuelan Llanos foothills as interpreted by Duerto et al. (1998; Fig. 7). These flexural scarps grow at the front of active fold- and-thrust belts where deformation is dominated by thin-skinned tectonics, though all ramps are ultimately rooted under the Andes (overall thick-skinned tectonics). The thrusts at upper levels are gently dipping and form both flats and ramps (Fig. 7).

In spite of the thickness difference of the sedimentary sequences involved in thrusting in both flexural basins (two to three times larger in the Maracaibo basin than in the Barinas–Apure basin) and number of decollements (southeastern foothills shows only a major decollement level within the Pagüey Formation of Middle Eocene age whereas the northwestern one contains three), both foothills where triangular zones have developed, display many structural similarities (Fig. 4a,b). Similarities include: (a) intracutaneous wedges verge basinward; (b) the Tertiary sequence essentially is decoupled from the basement by a basinward detachment; (c) the intracutaneous wedges containing thrust sheets of basement rocks are overriden by the Tertiary sequence above chainward passive roof backthrusts; (d) within the Tertiary sequence, small triangular zones form between opposite-vergent thrusts; (e) foreland verging ramps crop out above shallower triangular zones; (f) Piggy-back basins, which are completely decoupled from the underlying sequences, are created between the shallower triangular zone and the range; and (g) both basins contain synorogenic mollasic sequences.

Since structural styles of deformation along both mountain belt edges are similar to a certain extent, the radical difference in overall shape between both flexural basins needs to be related to either the chain load itself or the effective elasticity of the lithosphere. For the MA, these two causes are added because the Maracaibo crust is much thinner than the SA crust, as discussed later. The Maracaibo basin is a rather narrow and short but deep depocenter. Instead, the Llanos flexural basin is long, wide and shallower. This flexural basin geometry directly responds to chain load on top of the overriden basement. When the mountain belt is loading over a large area of the basement, the resulting flexural basin is wide and shallow. On the contrary but under the same load, when loading is much localized on the edge of the overriden basement, the basin has to be narrow and deep. This effect is accentuated because the more localized load actuates on a thinner crust.

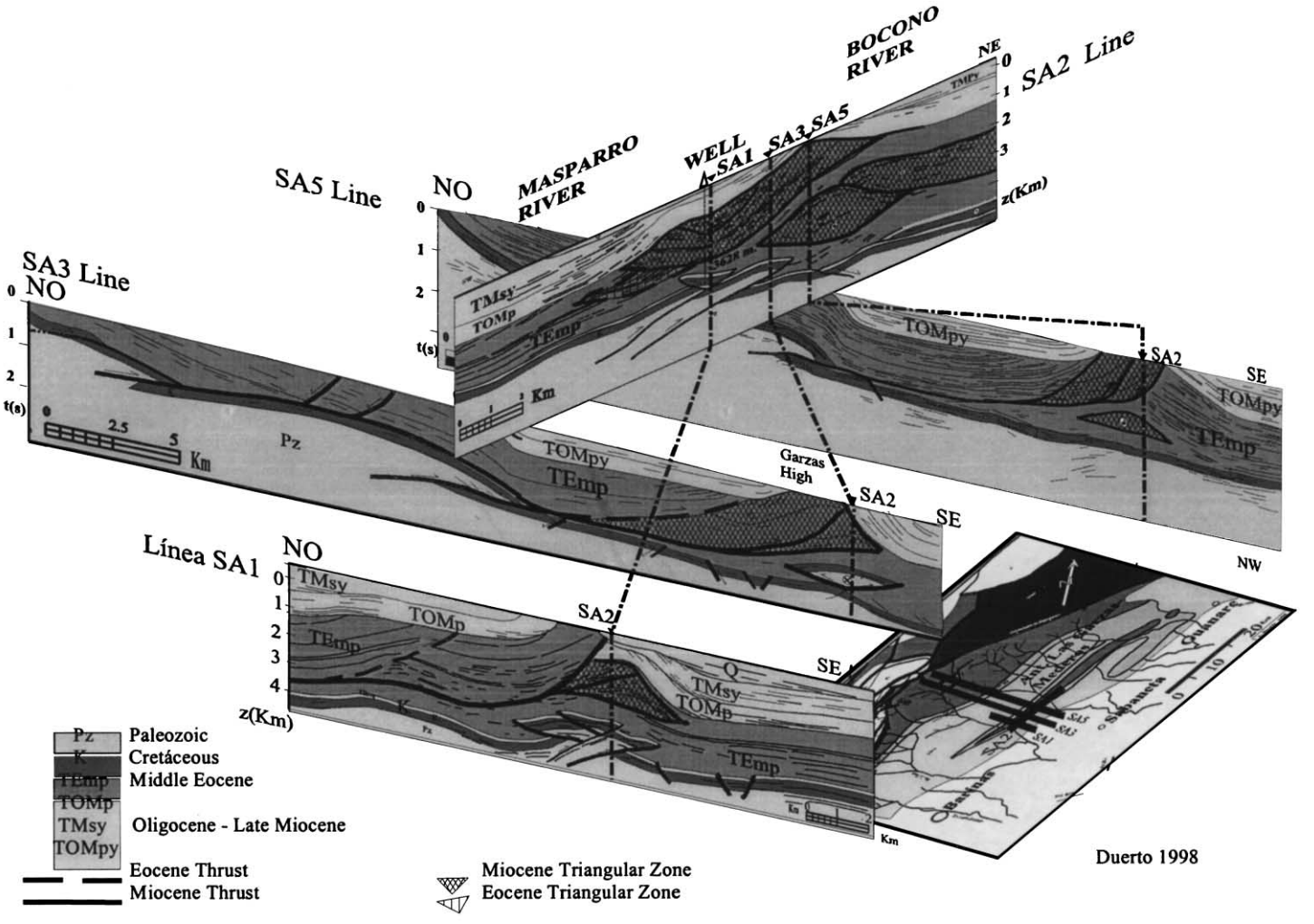

Fig. 7. 3D profiles of the southeastern Mérida Andes foothills across Las Garzas anticline, located between Barinas and Guanare (after Duerto, 1998), displaying active flat-ramp thrust faults, triangular zones and associated piggy back basins filled by Late Miocene–Quaternary mollasic deposits. Notice that flat-ramp structures, although nicely developed within the Tertiary sedimentary sequence of the Barinas–Apure flexural basin (thin-skinned tectonics), are rooted in the basement (thick-skinned tectonics).

Consequently, the shape of the related flexural basins suggests that the deeper structure of the MA chain is asymmetric, where the major northwestern bounding reverse fault needs to dip steeper that its SE counterpart, as proposed by Audemard (1991) and Colletta et al. (1997). Another implication also comes out—the MA is more overthrusted to the SE than to the NW.

8. Seismicity and focal mechanisms

The Boconó fault zone has been cited as responsible for most of the largest MA earthquakes, as Rod (1956a) has initially stated. Cluff and Hansen (1969) have also expressed the same conviction for both historical and instrumental earthquakes (refer to pages 5–13 through 16, and 5–45). Among the large historical earthquakes in the MA, Cluff and Hansen (1969) have ascribed the 1610, 1812, 1894, 1932 and 1950 earthquakes to the Boconó fault. Besides the 1610, 1812 and 1894 events, Aggarwal (1983)—later cited textually by McCann and Pennington (1990) and Suárez and Nábelek (1990)—also ascribed the 1644 and 1875 earthquakes to the Boconó fault. Seismotectonic associations of a few of these are still uncertain. For instance, Grases (1990) indicates a probable association of the Tocuyo 1950 earthquake with the Boconó fault, as Cluff and Hansen (1969) did. But

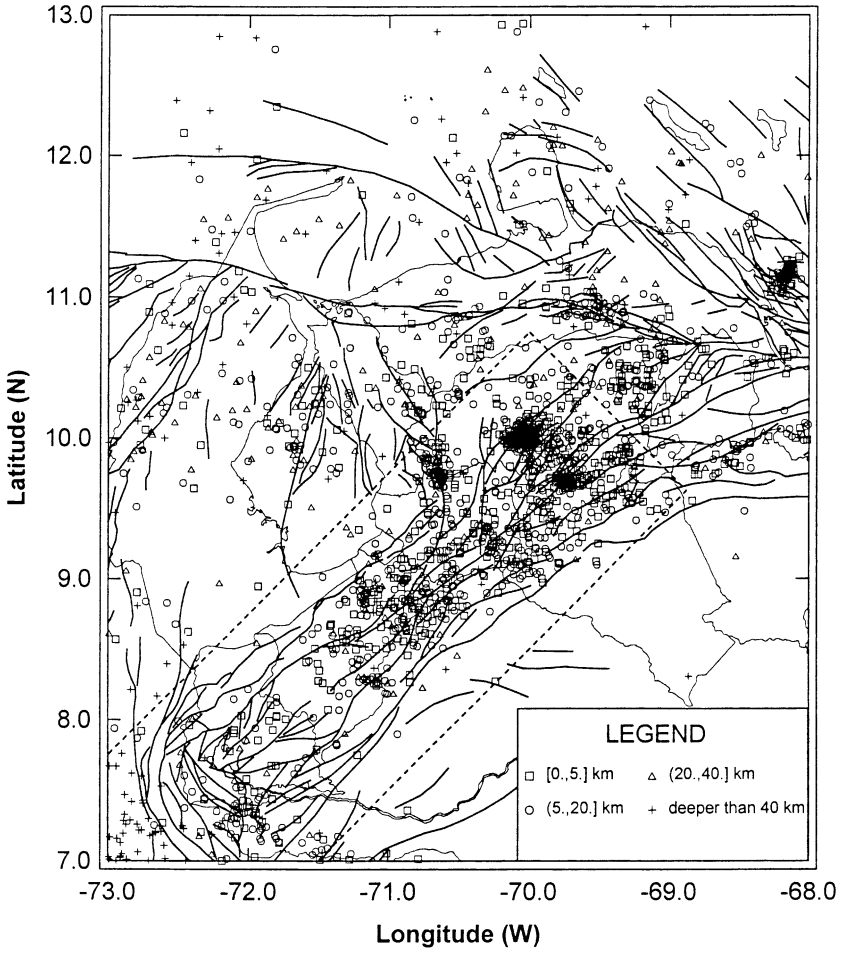

Fig. 8. Instrumental seismicity of the Mérida Andes for the period 1983–1999. Notice that most events are shallow, restricted to the upper-seismogenic or brittle-crust and bounded by both foothills thrust systems (after Funvisis catalog).

Choy (1998) and Audemard et al. (1999b) propose that other neighboring faults are potential sources because of the structural complexity in the epicentral region, located west of the Boconó fault (Fig. 3). Furthermore, Singer and Beltrán (1996) associate the 1644 Pamplona and 1875 Cúcuta earthquakes with the Pamplona indenter, and the 1644 event particularly with the Aguas Calientes fault and not with the BF. Conversely, the association of the 1610 and 1894 earthquakes with the southern segment of the Boconó fault has been recently confirmed by paleoseismic studies (Audemard, 1997a).

The present-day seismicity along the Boconó fault occurs within a broad zone, involving the entire width

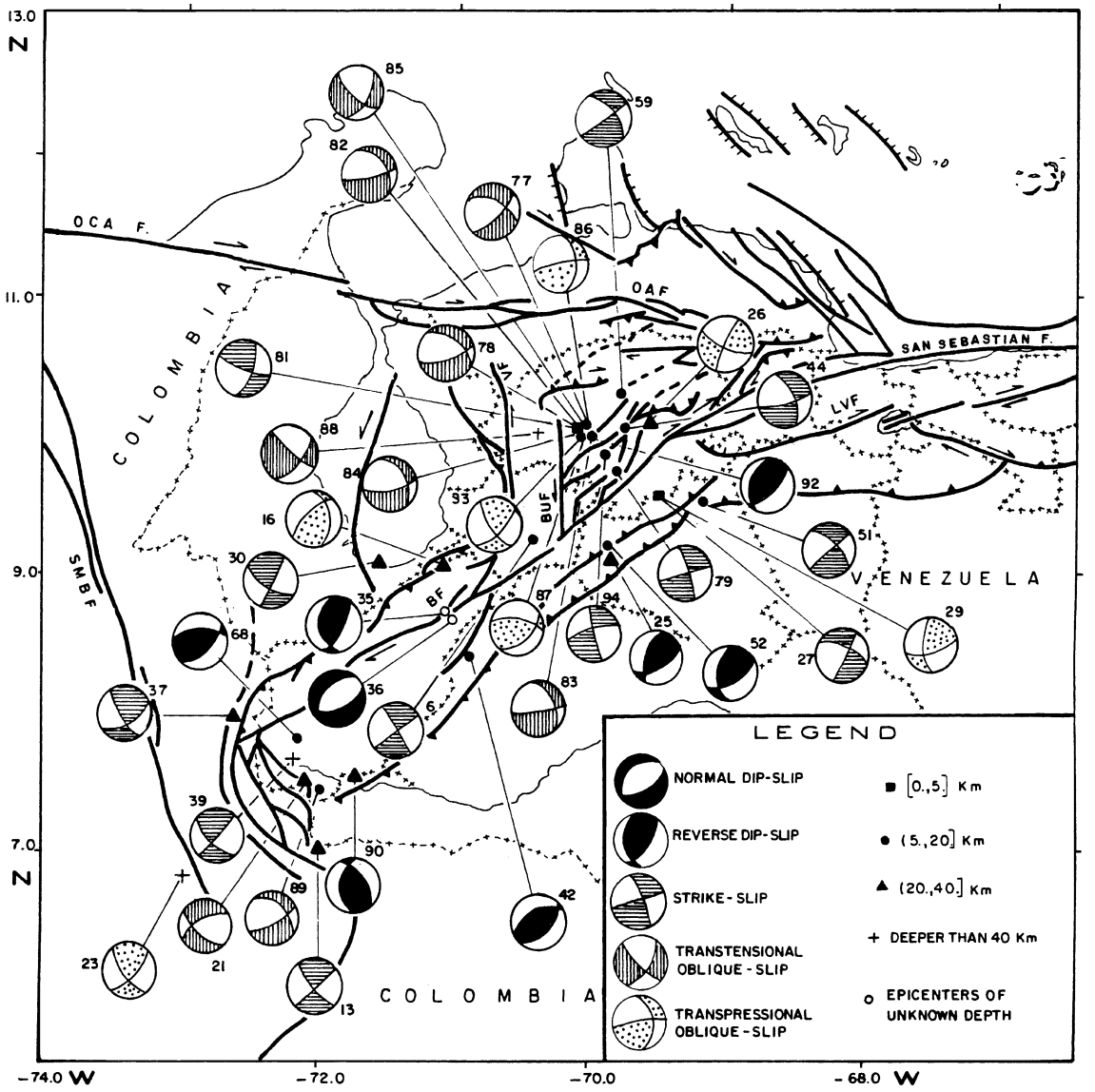

Fig. 9. Focal mechanism solutions for earthquakes located within or near the Mérida Andes, indicating the corresponding depth of the event (modified from Audemard et al., 1999b). Solutions are gathered based on their dominant slip. Trajectories of σ_{Hmax} displayed in Fig. 2 are partly derived from these focal mechanism solutions, which agree rather well with slip determined by neotectonic studies.

Table 1
Parameters of focal mechanism solutions for earthquakes within or near the Mérida Andes (from Audemard et al., 1999b)

Date (year/month/day)	Latitude (°)	Longitude (°)	Focal depth (km)	Magnitude	Nodal Plane A			Nodal Plane B			*T* axis		*P* axis		Label number
					AZI	DIP	RAKE	AZI	DIP	RAKE	AZI	DIP	AZI	DIP	
65/07/19	9.25	70.44	20.0	5.2	55	90	180.0	145.0	90.0	0.0	190.0	0.0	280.0	0.0	**6**
67/12/21	7.00	72.00	29.0	4.0	138	76	0.0	48.0	90.0	166.0	2.1	9.8	93.9	9.8	**13**
68/05/13	9.06	71.10	29.0	4.9	228	60	130.9	348.0	49.1	41.4	191.3	54.7	290.2	6.3	**16**
70/01/27	7.49	72.09	31	5.6	240	60	−143.9	130	59.4	−35.5	4.9	0.4	95.3	45.6	**21**
73/07/08	6.80	73.00	156.0	5.4	44	64	154.1	146.0	66.9	28.5	5.8	36.0	274.5	1.9	**23**
75/03/05	9.13	69.87	25	5.6	210	50	56.4	76	50	123.4	52.6	64.9	143.1	0.2	**25**
75/04/05	10.10	69.60	36.0	5.5	112	80	168.6	204.0	78.8	10.2	67.9	15.1	158.1	0.8	**26**
75/04/05	9.56	69.52	2.0	5.5	294	68	0.0	204.0	90.0	158.0	156.8	15.4	251.2	15.4	**27**
77/12/11	9.56	69.52	2.0	5.5	70	65	139.3	180.0	53.7	31.6	30.2	45.8	127.3	6.9	**29**
79//05/05	9.09	71.56	22	5.6	119	53	5	26	86	142.9	335.8	28.3	78.5	22.1	**30**
80/01/02/C[a]	8.71	71.08			29	65	103.2	180	28.1	63.9	323.7	67.3	109.2	19	**35**
80/01/02/C[a]	8.66	71.03			221	30	−106.6	60	61.4	−80.6	143.1	15.9	351.9	72	**36**
80/11/26	7.96	−72.62	40	5.2	57	64	170.9	151	81.9	26.3	17	24.2	201.4	12.1	**37**
82/07/04	7.65	72.19	53.5	5.5	136	66	4.9	44.0	85.5	155.9	357.4	20.1	92.4	13.4	**39**
84/C[a]	8.4	70.9	<20	<4	45	44	77.6	242	47.3	101.7	222.9	81.3	323.7	1.7	**42**
84/06/14	10.05	69.78	18	5.2	340	65	−11.7	75	79.4	−154.5	205.4	9.7	300	25.4	**44**
86/C[a]	9.5	69.2	<20	3–4.0	315	60	0	225	90	150	175.9	20.7	274.1	20.7	**51**
86/C[a]	9.2	69.9	<20	<4.0	190	40	52.5	55	59.3	117	13.3	64.5	125.9	10.4	**52**
88/C[a]	10.3	69.8	<20	<4.0	325	55	0	335	90	145	184.3	23.9	285.7	23.9	**59**
89/01/30	7.80	72.17	11.2	4.4	46	50	58.2	270.0	49.4	122.2	157.9	0.3	248.6	66.2	**68**
91/08/07	9.99	69.992	18.2	5	45	70	−141.9	300	54.6	−24.8	169.4	9.7	267.8	40.7	**77**
91/08/17	10.003	70.032	16.2	5.3	310	45	−35.8	67	65.6	−129.1	184.1	12	290.1	52.4	**78**
91/08/17	9.74	69.83	15	5.5	344	86	0	74	90	−176	200.9	2.8	299.1	2.8	**79**
91/08/20	10.05	70.10	1.8	4.5	19	68	174.7	111.0	85.1	22.1	337.1	19.0	243	11.8	**81**
91/08/20	10.054	70.105	1.8	4.5	331	42	−18.5	75	77.7	−130.5	194.7	22	306.5	42.5	**82**
91/08/20	9.988	70.014	18	4.2	345	40	−10.4	83	83.3	−129.5	203.5	27.4	317.8	38.6	**83**
91/08/21	10.038	70.032	15.1	4.5	75	75	−126.9	326	39.5	− 24	192.1	21.3	306.6	46.8	**84**
91/08/21	10.03	70.03	15.1	4.5	30	55	−20.3	132.0	73.5	−143.2	256.4	11.8	356.5	37.4	**85**
91/09/02	10.063	70.032	7.9	4.7	0	45	12.6	261	81.1	134.3	209.5	37.5	318.6	23	**86**
91/09/14	10.021	70.041	9.3	4.1	280	65	123.1	43	40.6	40.5	234.7	56.7	346.6	13.8	**87**
91/09/14	10.02	70.41	41.0	4.1	37	−6	−6.0	130.0	84.8	−149.0	259.7	16.8	357.7	24.7	**88**
94/05/31	7.423	72.001	13.5	6.1	63	75	−128.5	315	40.9	−23.3	181.1	20.6	293.8	45.8	**89**
94/11/09	7.53	71.73	21.3	5.2	178	42	112.4	329	51.8	71.1	100.7	74.4	72.3	5	**90**
95/12/29	9.99	70.08	16.2	5.1	47	65	103.7	197	28.3	63.1	342.6	67.1	126.8	18.9	**92**
95/12/29	9.99	70.08	16.2	5.1	47	65	155.3	148	67.7	27.2	8.2	34.5	277	1.8	**93**
95/12/31	9.86	69.91	15	5.1	257	74	−176.4	166	86.5	−16	212.6	8.7	120.4	13.8	**94**

[a] Composite focal mechanism.

of the MA, suggesting that other faults may be seismogenic as well (Fig. 8). For instance, the Guanare March 05, 1975 and the Ospino December 11, 1977 earthquakes of magnitudes mb 5.5 and 5.6, respectively, are the most recent and largest events associated with the Southern Andean Foothills thrust system (Piedemonte Oriental fault). The depth distribution of seismicity associated with the chain build-up demonstrates that the entire (first 20–25 km) brittle crust is being deformed at present (Fig. 8).

Earthquake focal mechanism solutions constrain present fault kinematics. Besides, the individual stress tensor derived from each solution matches well with the stress field presented in Fig. 2, where the east–west oriented σ_{Hmax} in the southern MA progressively changes to a NW–SE orientation towards the north along the chain. Though the number of focal mechanism solutions is not large (Fig. 9 and Table 1), it distinctly shows the active strain partitioning. The focal mechanism solutions also confirm fault-slip determinations based on geologic criteria since they locally exhibit mainly pure strike and reverse slip.

Focal mechanism solutions for the MA and neighboring regions (Fig. 9) compiled by Audemard et al. (1999b) are distributed as follows: (a) 12 out of 36 solutions exhibit dextral slip on NE–SW trending nodal planes that could be associated with the Boconó fault or other subparallel faults; (b) nine of them correspond to transtensional oblique slip; (c) seven solutions display transpressional oblique slip; (d) seven displays almost pure reverse dip-slip solutions, spread over the mountain belt; and (e) only one shows extensional dip-slip on normal faults paralleling and along the axis of the chain that could result from mountain spreading.

The seven transpressional oblique slip solutions are here discussed in detail because of the implications they have on constraining the direction of underthrusting and the strain partitioning mechanism occurring within the chain. Out of those seven focal mechanisms, only two (solutions 16 and 29) are relevant to this study because they are within the MA. Among the others, four solutions correspond to shallow moderate earthquakes that are in the Curarigua–Arangues region and located northwest of the MA. The fifth solution has its epicenter located in the northeastern EC. The two solutions of interest correspond to earthquakes with epicenters lying on the two opposite MA flanks. On the northwestern MA front, a 4.9 magnitude earthquake occurred in May 13, 1968 at a depth of 29 km (Pennington, 1981; Audemard et al., 1999b). The one occurring on the other foothills happened in December 11, 1977 at a depth of only 2 km (Audemard et al., 1999b). Consequently, very little transpressional oblique slip takes place within the MA chain and partitioning seems to be the actuating mechanism in the mountain belt. Thus, deformation models must satisfy the following three conditions. (1) Seismogenic deformation involves the entire brittle crust, and the Boconó fault cuts across the entire brittle crust to achieve partitioning. This condition has been fulfilled in some models (Castrillo, 1997; and all MA positive-flower structure models). (2) If any type-A subduction is to be proposed under the MA, no subduction slab penetrating the mantle is supported by present seismicity. This precludes any advanced stage of continental subduction and requires deformation to remain at crustal levels. (3) The lack of transpressive oblique slip (where a single structural feature should show simultaneously reverse and along-strike slips) within the MA, as evidenced by the focal mechanism solutions, discards any model that calls on transpressional brittle features into the crust, as requested by the models proposed by Kellogg and Bonini (1982), Audemard (1991), De Toni and Kellogg (1993), both models by Jácome (1994) and Colletta et al. (1997).

Some intermediate earthquakes, up to 200 km deep, have been detected under lake Maracaibo basin (Fig. 8; some of those marked by crosses). They have been attributed by mean of focal solutions (e.g., Dewey, 1972; Kellogg and Bonini, 1982; Malavé and Suárez, 1995; Pérez et al., 1997) and seismic tomography (Van der Hilst, 1990) to the SSE-directed oceanic slab of the LAS or its western extension that bends around northwestern SA until it strikes north–south and gently dips east in Colombia.

9. Shortening vs. wrenching

9.1. Amount

Ratio of shortening to wrenching may give us clues about the significance of both deformation processes in the Andean orogeny. Audemard (1991) indicates that the southernmost Venezuela Andes has undergone

a 14% shortening, of about 12 km, which should be considered as a lower bound. He also indicates that shortening across the Avispa massif (further northeastward; Figs. 3 and 6) would be of the order of 45 km (40%). Besides, the same author suggests that reconstructions across other portions of the Andes would lead to larger estimates. In fact, Colletta et al. (1997) derive shortening values that average 60 km. These values strongly depend on thrust dips, which are not well constrained at depth. Besides, accurate estimates of shortening are hard to get because newly formed shortcut low-angle thrust faults are supposed to also accommodate part of it. This latter mechanism has been proposed by Colletta et al. (1997). However, a fundamental question needs to be raised about these faults actually being shortcut faults instead of high-angle reverse thrust faults later flattened (originally over 40–50° dip Jurassic normal faults)? Some discussion on the model proposed by Colletta et al. (1997) may offer some additional constraints on the reliability of their estimate based on reconstruction of balanced cross-sections. The following observations can be derived from their Plate 1: (a) the dip of the graben-bounding faults in their restored section (Jurassic stage) is rather low and the graben is obviously asymmetric where NW-bounding faults consistently show steeper dips. They insinuate that the Jurassic rifting was generated by a kind of simple shear model since they define a major NW-dipping, low-angle, normal fault in both restored sections. This Jurassic structuration has fundamental implications in the future tectonic inversion of the graben; (b) most crustal-scale reverse fault planes flatten when reaching upper crustal levels, which could be produced by topographic flattening of the chain due to gravity. This overestimates the amount of shortening.

A very rough estimate of shortening can be derived from considering that the chain core exposes metamorphic and igneous rocks of continental crust origin at about 5000 m above sea level. Therefore, a maximum total uplift of the order of 12–15 km can be reasonably proposed. Assuming that the Jurassic faults had original dips of the order of 30°—which is rather low for a normal fault—the total shortening neglecting any internal ductile deformation would be of some 40–50 km at most from simple trigonometric calculations. Therefore, estimates of 60 km might be overestimating the amount of shortening in some 20–25% because mountain belt flattening has not been taken into account.

As much as 70–80 km of dextral wrench offsets in Mesozoic rocks have been measured along the Boconó fault (Stephan, 1982). This value has been disputed by Audemard (1993) based on the reliability of subhorizontal geologic markers for measuring horizontal displacements. More reliable and frequent dextral offsets are of the order of 30 km (Giraldo 1989; Audemard and Giraldo, 1997). An additional argument in favor of the total right-lateral slip along the Andes axis may be derived from present location of Bouguer anomaly minima in both flexural basins. The southeastern foothills minimum is located between Capitanejo and Ciudad Bolivia (refer to gravimetric map by Bonini et al., 1977), exactly SE of the highest peaks of the Sierra Nevada, the latter in turn being south of the Boconó fault (in the southeastern half of the MA). Conversely, the northwestern foothills minimum is located near Caja Seca–Bobures (Fig. 3 for relative location), being shifted northeastward 30 km with respect to both the other flank gravimetric minimum and the highest peaks of the MA.

Consequently, a wrenching/shortening ratio of 1:1 to 1:1.5 cannot be neglected: 30 km of dextral wrenching against a shortening amount of the same order or under 50% higher (40–50 km). This poses a problem for models proposing a high-dip Boconó fault plane that dies out at upper crustal levels or roots on thrust faults within the brittle crust (i.e. Fig. 44 of Audemard, 1991; Fig. 10 of Kellogg and Bonini, 1982; Fig. 18b of De Toni and Kellogg, 1993; Fig. 6-6 of Castrillo, 1997; plate 1 of Colletta et al., 1996, 1997). The lack of transpressive oblique slip within the chain, as evidenced by the instrumental seismicity, requires that the Boconó fault reaches the lowermost brittle crust at least and roots on an aseismic structure as a lower-crustal detachment at the rheological brittle–ductile transition in the crust to allow partitioning, as proposed by Audemard (1991).

9.2. Activation age

The age of onset of chain uplift has been determined by different approaches and techniques. Most agree that the MA started to build up sometime in the Late Miocene (e.g., Stephan, 1982; Audemard, 1991, 1993;

Colletta et al., 1997). The age of sedimentary growth wedges in both flanking flexural basins support this (Audemard, 1991; De Toni and Kellogg, 1993; Duerto et al., 1998). Uplift ages derived from apatite fission-tracks by Kohn et al. (1984) and Shagam et al. (1984) support the sediment-derived ages but also suggest uplift diachronism across the MA from southeast to northwest. This diachronism will be discussed later because of its implications for a proposed model.

On the other hand, a reliable age of wrenching onset within the chain is not available because of lack of thorough sedimentary records for any of the pull-apart basins associated with the Boconó fault. Therefore, it has to be derived indirectly based on certain assumptions. For instance, Audemard (1993) proposed that RLSS within the MA is a direct consequence of the suturing related to the PA collision. This collisional process started at about 12 Ma and a land bridge was achieved by 3 Ma. Another approach is by considering that the entire northwestern corner of SA (including most of the Ecuadorian, Colombian and part of the Venezuelan Andes) is split from cratonic SA by a long, complex dextral transform fault system, including the Pallatanga, Algecira, Guaicaramo, Boconó and other minor faults (Case et al., 1971; Dewey, 1972; Pennington, 1981; Stephan, 1982; Audemard, 1993, 1998; Freymueller et al., 1993; Ego et al., 1996). The opening and deepening of the Jambelí graben in the gulf of Guayaquil, offshore Ecuador, is related to the northward escape of northwestern SA (Audemard, 1993, 1998; Figs 1 and 2). This basin, interpreted as a pull-apart, is mainly filled by Plio–Quaternary marine deposits, but sedimentation started in the Late Miocene (Benítez, 1986), thus constraining the initial age of wrenching (Audemard, 1993). This would also imply that a second continental block—bounded by the LLSS Romeral fault system and the oblique slip EC Southern Foothills fault system—is being extruded northward as well but at a lesser rate, which may be supported by offsets of the LAS front north of the city of Santa Marta (Fig. 2). Consequently, the Santa Marta–Bucaramanga fault is simply accommodating the differential slip rate of escape between the MTB and the block located south of it and bounded by the Romeral and the EC Southern Foothills fault system.

Therefore, thrusting, transcurrent slip and chain uplift in the MA seem to start at once at the end of the Miocene, thus implying that the occurrence of partitioning is related to a single cause—the present stress tensor that results from major tectonic plate interactions (Fig. 2).

10. Discussion

For almost two decades, geoscientists have tried to explain the MA orogeny by means of the continental subduction model proposed by Argand (1924). The ambiguity and large diversity of crustal models results from the lack of reliable data constraints at crustal scale such as deep seismic reflection profiling. The data previously discussed in this paper shows that the MA behaves differently both along strike and transversely to the range.

Several models propose that the crust of the Maracaibo basin underthrusts (e.g., Kellogg and Bonini, 1982) or incipiently subducts (e.g., Colletta et al., 1997) beneath the SA continental crust to explain the development of a deeper flexural basin along the northwestern flank of the chain. Besides, most of these SE-directed continental subduction (underthrusting) models regarding how the MA are conceived do not take into account the significant wrenching accommodated within the mountain belt by the Boconó fault (i.e., Kellogg and Bonini, 1982; Colletta et al., 1997), which is driving the NNE extrusion of the Maracaibo block with respect to SA. This fact was first pointed out by Schubert (1985) regarding Kellogg and Bonini's (1982) model. Wrenching along the chain axis of at least as much as half of shortening across the MA necessarily needs to be taken into consideration. Moreover, activation of wrenching and shortening in the Andes seems to be coeval, meaning that strain partitioning started in the Late Miocene–Early Pliocene and is still going on. On the other hand, models proposing a Boconó fault bounded to the upper crustal levels would require that the deeper part of the continental subduction slab (or crustal thrust fault in other models) east of the Boconó fault exhibited oblique (both reverse and right-lateral) slip within the seismogenic crust, which is not attested by any focal mechanism solutions calculated for earthquakes recorded on the eastern side of the MA or under the Llanos basin, although it may be argued that the present recording period is too short. However, strain partitioning seems to be the actuating mechanism, as stressed by Colletta

et al. (1997) but lacking to propose a coherent model. Moreover, the two only focal mechanism solutions (labelled 16 and 29) within the mountain belt exhibiting transpressive oblique slip would rather support a NW dipping plane, since the deeper −29 km-event lies under the northwestern foothills and the other event located under the opposite foothills is very shallow (only 2 km deep). This would clearly favor an incipient NW dipping continental subduction or low-angle NW-dipping underthrusting.

Complementary evidence of ongoing uplift in the MA is brought by the development of Quaternary staircased alluvial terrace systems along major rivers and extremely quick downcutting of rivers revealed by the narrow V-shaped cross profile of these rivers.

Tectonic inversion very frequently reutilizes favorable preexisting weakness zones. Therefore, it is not clear why the major low-angle normal fault shown in the Plate 1 of Colletta et al. (1997) is not reutilized during inversion but the minor antithetic normal fault was. If their proposed major MA structure happens to be correct, NW-dipping underthrusting seems a more plausible process during tectonic inversion. Suggesting that the major normal faults during the Jurassic rifting should have dipped outward around cratonic areas seems to be in accordance with the structuration of a passive margin around the northern edge of the SA craton, as Colletta et al. (1997) did.

Several other problems are encountered when evaluating these SE dipping subduction (or underthrusting) models regarding: (1) northeastward extension of this Maracaibo-related slab beyond the left-lateral Valera fault, if the MA northwestern foothills corresponds with its surface expression (Figs. 1 and 3); (2) general organization and interaction within the upper mantle between the LAS and the proposed MA subduction slabs somewhere beneath Lara and Yaracuy states, if the SE dipping subduction prolongs as far north; and (3) role played by the Valera fault in this active tectonic setting because the northwestern flexural basin ends against it.

Consequently, taking into account the above-mentioned limitations of those SE dipping continental subduction (or underthrusting) models, then let us evaluate the NW-dipping continental subduction models, though crustal flower-structured models may not be ruled out. These latter models could be adapted to the data by just considering the chain asymmetry, which is inherited from the original Jurassic graben geometry.

From the rheological viewpoint, the subduction of an older, thicker and consequently colder and heavier cratonic crust under a younger, thinner, and consequently hotter and lighter continental crust is a normal setting (Mattauer, 1983, 1985; Shemenda, 1993; Mattauer et al., 1999). The Maracaibo subducting crust has undergone a more recent tectonic and thermal event due to continental rifting during the Jurassic than the long-cooled Precambrian crust of SA craton, which should impose some bouyancy to the Maracaibo crust with respect to surrounding "stable" cratonic areas, preventing it to sink under SA craton. Moreover, a thinned continental crust is weaker than normal continental crust, being more susceptible to deformation (Taboada et al., 2000), which makes underthrusting more difficult. Recent deep refraction studies show that the SA craton Moho is 44–47 km deep in the northern Guiana shield (Schmitz et al., 1999; Chalbaud, 2000; Chalbaud et al., 2000), compared to the 29 km thick Maracaibo crust (Padrón and Izarra, 1996). Besides, the cratonic Mohorovicic discontinuity sinks to the west (towards the MA), exhibiting the deepest Moho just east of the Orinoco river, on a 600-km-long west–east profile (Schmitz et al., 1999; Chalbaud, 2000; Chalbaud et al., 2000). Then, the MA is sitting along the juxtaposition of two very different continental crusts where the Maracaibo crust is the weaker, hotter and thinner.

The sinking to the NW of a continental slab along the southeastern edge of the MA would not produce much interference with the gently south-dipping oceanic LAS of northwestern Venezuela, since both incipient subducting plates show opposite vergence although they are called to converge under the Maracaibo basin. Besides, this geometric configuration would also favor a certain mechanical and kinematic continuum between the MA and the Caribbean nappes of the Coast range. In some way, it may suggest that the NW-dipping oblique subduction of northern SA passive margin under the Caribbean plate in the Paleogene along northern Venezuela—which later evolved successively into an oblique collision and a transpressional boundary (Audemard, 1993)—has been transferred southwestward much later, from the front of the SSE-vergent Caribbean nappes in central Venezuela to the southeastern MA flank. The major boundary prolonged

from the nappes front into the southeastern bounding fault of the Jurassic graben (corresponding to the major extensional feature of Colletta et al., 1997 in their restored sections) that later resulted in the present Venezuelan Andes (MA), as attested by active NE–SW trending subsurface compressional structures in the Guarumen area (Blin, 1989).

Ages of cooling derived from apatite fission tracks by Kohn et al. (1984; Fig. 12) also bring additional supporting evidence in favor of a NW dipping continental subduction. They deduced from cooling ages that the southeastern MA flank raised later than the west one that started uplifting in the Late Miocene. They also suggested that this would need some kind of underthrusting (subduction?) along the southern flank of the Andes. This diachronism might be related to the original Jurassic graben asymmetry. Since faults dip higher in the northwest than in the southeast, uplift is more efficiently and fast achieved where inversion is controlled by higher-angle reverse faults and a certain delay in between takes place before it also occurs on the other chain flank. Another possible explanation to the uplift diachronism transversely to the mountain belt could be related to partial locking of progression of the intracutaneous basement-thrust-sheeted wedge into the Maracaibo Tertiary sequence in the Late Miocene–Early Pliocene. Later, as a consequence of continued compression across the Andes, uplift resumed or progressed on the west flank of the MA, which might explain why Las Virtudes out-of-sequence thrust in the central MA is destroying at present the triangular zone by overthrusting, whereas the intracutaneous wedge and triangular zone are still preserved in the southern portion of these western foothills where shortening across the Andes seems less important (in the order of 12 km after Audemard, 1991).

Based on all the arguments and supporting evidence discussed along this paper, it is herein proposed that the MA is mechanically functioning as a brittle-crustal stacking wedge, which is partly decoupled from the ductile crust by a detachment, similarly to the proposal of Mattauer (1983, 1985) for the Himalaya, though in that case, the entire crust is being involved and decoupled from the mantle. Then, the crustal wedge builds up by inside folding and thrusting between a major gently NW dipping thrust (low-angle underthrusting or incipient type-A subduction) and an antithetic steeper SE dipping crustal backthrust, which loads the Maracaibo block (comparable to analogue modelling of sedimentary accretionary wedges with high basal friction law). Internal brittle deformation of the wedge is driven by preexisting structures, thus slightly differing from a sedimentary prism in that respect. Besides, internal structure of the chain varies along strike as discussed in Section 5. Fig. 10 only displays the major southern MA structuration—which looks internally much different to a sedimentary accretionary wedge with high basal friction law—where the Pamplona indenter structuration (dominant high-angle NW-vergence) is superimposed. Consequently, both flexural basins may be compared to a fore-arc basin (Maracaibo basin) and to a foredeep (Barinas–Apure basin), thus explaining the difference in depth and size between the two basins and thickness of involved sedimentary sequence. Simultaneously, the crustal wedge is split into two by a subaxial wrench system, thus allowing the escape towards the NNE relatively to SA of the western half of the MA along with the MTB, which is delaminated along the brittle–ductile crust boundary or within the ductile crust (Fig. 10). In this case, no seismicity is to be envisaged below the crust seismogenic zone. Assuming that the 29-km-deep 1968 earthquake—whose epicenter lies on the northwestern MA flank (refer to Section 8)—is actually occurring on the underthrusting plane, the dip of the incipient NW-dipping continental subduction would be of 17°, mirroring the dip of the southwestern portion of the LAS.

Some analogies to certain extent with respect to some mechanic and kinematic processes can be put forward between the geodynamic setting of northwestern Venezuela and the India–Eurasia collision and related block extrusions, although the main differences between both regions, besides size of deformation belts, reside in: (a) the involved thickness in both regions—India–Asia collision affects the entire lithosphere (Mattauer, 1983, 1985; Mattauer et al., 1999), whereas it only essentially involves the brittle crust in northwestern Venezuela (this paper)—and (b) the cumulative shortening accommodated in both cases has no possible comparison. However, in both regions, an old, heavy and cold cratonic lithosphere subducts a younger, lighter and heated continental lithosphere, inducing both shortening (orogeny) in the hangingwall block (Andes on one case and Himalaya and Pamir–

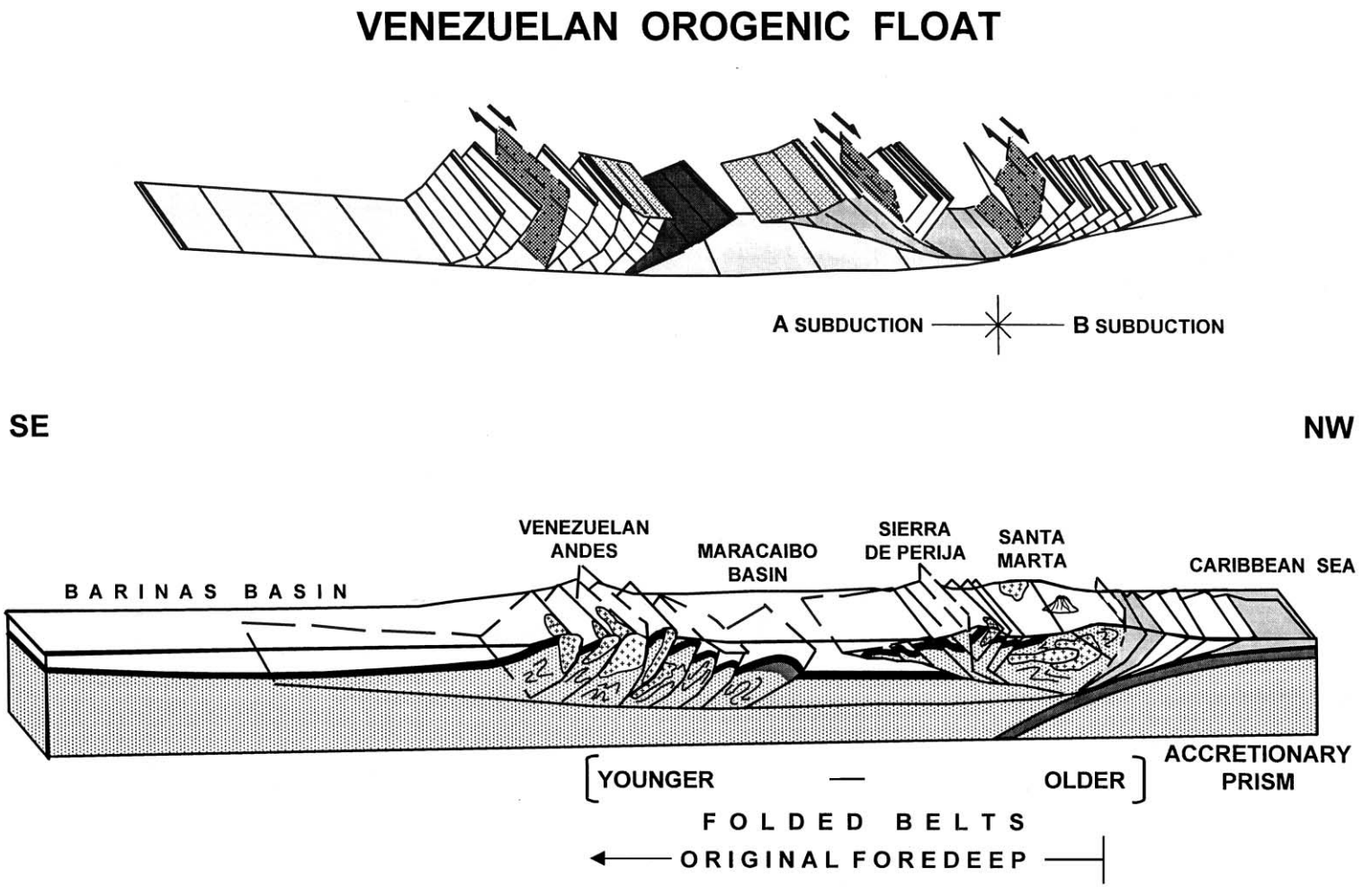

Fig. 10. The Mérida Andes in relation to an orogenic float model. Cross-section extends from the northwestern tip of the Santa Marta Block (SMB; location in Fig. 1) to the Llanos Basin, across the southernmost Mérida Andes, at the Pamplona indenter. Bottom figure displays major geologic units and structures, whereas top figure only exhibits major structures—brittle thrust and strike-slip faults, detachments and triangle zones—to give a more legible view of their interplays.

Kunlún in the other one) and lateral extrusion of continental masses (Maracaibo triangular block in Venezuela and Indochina and South China in Asia) because of the difficulty of one continental plate of sinking under another one, which induces the formation of a type-B subduction on its outer edges (LAS in Venezuelan case and west Pacific subduction in the Far East). On the other hand, India acts as an indenter (Tapponnier and Molnar, 1976; Peltzer and Tapponnier, 1988) and so does the Guayana shield margins at the Colombo–Venezuelan border (southern MA; Boinet, 1985; Boinet et al., 1985), though scaling is not comparable because amount of shortening is huge and continental subduction is at a very advanced stage in the India–Asia collision whereas it is just beginning in the eastern Andes foothills (no actual continental slab exists yet—crustal delamination is accounting for some thickening of the crust under the MA—and shortening is less than 60 km). Southern Venezuelan Andes indentation seems to mirror into the northern segment of the Eastern Cordillera of Colombia across the Santa Marta–Bucaramanga fault, all showing a huge propeller-like shape centered upon the Santa Marta–Bucaramanga fault.

11. Conclusions

Ambiguity among the Mérida Andes models (from crustal-scale positive flower structures to either polarity type-A subduction) reveals the lack of deep seismic reflection data that would definitely constrain model proposals. However, taking into account all the recent available geological and geophysical (including seismological) data, some models seem to explain better the Mérida Andes build-up and present structure. For instance, the SE-dipping type-A subduction models exhibit important problems when geometric boundaries of the continental subduction, present seismic activity and their focal mechanism solutions along and across the chain are taken into consideration. With respect to models of the crustal flower-structure type, present data is insufficient to rule them out, and they might still be valid if tectonic inheritance would be incorporated. Nevertheless, we support models of the type involving incipient gently NW-dipping continental subduction, at a larger scale of the floating orogen type. In few words, the Andes of Venezuela are envisaged as a brittle-crustal stacking wedge that generates a shallow foreland basin on the foredeep side along the Llanos foothills, whereas it strongly flexes the Maracaibo block crust on the forearc-equivalent side where a deep flexural basin develops in association with a chain-scale backthrust along the Maracaibo foothills on the northwest. Both thrust fronts are masked by Neogene triangular zones, which grow on top of basement-involved thrust stacks (similar to an offscrapping bulldozer). Besides, the chain is split into two uneven halves—more marked in the southern Mérida Andes—by a major right-lateral strike-slip fault (The Boconó) located in the inner chain. This RLSS feature drives extrusion of the Maracaibo block to the north–northeast in combination with the Santa Marta–Bucaramanga fault in Colombian territory, while chain is shortened across in NW–SE direction.

From combining fission-track ages of uplift, major geodynamic considerations and Andes-related mollasic deposits on both foothills, thrusting, transcurrent slip and chain uplift seem to start at once, at the end of the Miocene, thus implying that the occurrence of partitioning is to be related to a single cause: present stress tensor that in turn results from major tectonic plate interactions. In fact, wrenching along the chain, of the order of 30 km on the Boconó fault, is as much as half of or similar to the transverse shortening distributed across the entire chain width. It is worth mentioning that the major present structure of this chain is highly controlled by preexisting structures (relevant structural inheritance).

Acknowledgements

Both authors wish to acknowledge their own institutions, PDVSA and FUNVISIS, respectively, for allowing this contribution. Our thanks also go to: Dr. Herbert Rendón, head of the Seismological Department of Funvisis, who prepared and provided the seismicity and focal mechanism figures; and our colleague Leonardo Duerto at Pdvsa's Exploration and Production Division for preparing and giving permission for publication of one of his own figures. We are grateful as well to the 4th ISAG organisers (Drs. Gerhard Wörner and Etienne Jaillard in particular) who encouraged this contribution and helped financing the

co-author's attendance through the French Ministry of Foreign Affairs. Final high-quality drafting is due to Marina Peña. This review paper was greatly improved from comments by Dr. James Kellogg and two other anonymous reviewers. Suggestions and comments from the Editor-in-Chief, Dr. Jean-Pierre Burg, gave the final shape to this contribution.

References

Aggarwal, Y., 1983. Seismic gaps and earthquake hazard in Venezuela. Proceedings of Simposio Neotectonica, Sisimicidad y Riesgo Geológico en Venezuela y el Caribe, Caracas. Funvisis, Caracas, p. 26 (abstract).

Argand, E., 1924. La tectonique de l'Asie. Congres Geolgique International, Liege 1922, 169–371.

Audemard, F.E., 1991. Tectonics of Western of Venezuela. PhD Thesis, Rice University, Texas, 245 pp + appendices.

Audemard, F.A., 1993. Néotectonique, Sismotectonique et Aléa Sismique du Nord-ouest du Vénézuéla (Système de failles d'Oca-Ancón). PhD Thesis, Université Montpellier II, France, 369 pp + appendix.

Audemard, F.A., 1997a. Holocene and historical earthquakes on the Boconó fault system, southern Venezuelan Andes: trench confirmation. Journal of Geodynamics 24 (1–4), 155–167.

Audemard, F.E., 1997b. Los Andes Venezolanos, visión alterna. VIII Congreso Geológico Venezolano, Porlamar, vol. 1. Sociedad Venezolana de Geólogos, Caracas, pp. 85–92.

Audemard, F.A., 1998. Evolution Géodynamique de la Façade Nord Sud-américaine: Nouveaux apports de l'Histoire Géologique du Bassin de Falcón, Vénézuéla. Transactions of the 3rd Geological Conference of the Geological Society of Trinidad and Tobago and the XIV Caribbean Geological Conference, Trinidad-1995, vol. 2. The Geological Society of Trinidad and Tobago, San Fernando, T&T, pp. 327–340.

Audemard, F.A., 1999. Morpho-structural expression of active thrust fault systems in humid tropical foothills of Colombia and Venezuela. Zeitschrift fuer Geomorphologie 118, 1–18.

Audemard, F.A., 2000. Major Active Faults of Venezuela. 31st International Geological Congress, Rio de Janeiro, Brazil. Brazilian Geological Society and others (extended abstract; CD-Rom format).

Audemard, F.A., Giraldo, C., 1997. Desplazamientos dextrales a lo largo de la frontera meridional de la placa Caribe, Venezuela septentrional. VIII Congreso Geológico Venezolano, Porlamar, vol. 1. Sociedad Venezolana de Geólogos, Caracas, pp. 101–108.

Audemard, F.A., Pantosti, D., Machette, M., Costa, C., Okumura, K., Cowan, H., Diederix, H., Ferrer, C., Sawop Participants, 1999a. Trench investigation along the Merida sectión of the Boconó fault (central Venezuelan Andes), Venezuela. In: Pavlides, S., Pantosti, D., Peizhen, Z. (Eds.), Earthquakes, Paleoseismology and Active Tectonics. Selected papers to 29th General Assembly, August 1997. Tectonophysics, vol. 308. Association of Seismology and Physics of the Earth's Interior (IASPEI), Thessaloniki, Greece, pp. 1–21.

Audemard, F.A., Romero, G., Rendón, H., 1999b. Sismicidad, Neotectónica y Campo de Esfuerzos del Norte de Venezuela. FUNVISIS' unpublished Report for PDVSA-CVP, Caracas, 221 pp.

Audemard, F.A., Machette, M., Cox, J., Dart, R. and Haller, K., 2000. Map and Database of Quaternary Faults in Venezuela and its Offshore Regions. US Geological Survey Open-File Report 00-0018. Include map at scale 1:2,000,000 and 78-page report.

Beck, C., 1985. Caribbean colliding, Andean drifting and Mesozoic–Cenozoic geodynamic evolution of the Caribbean. VI Congreso Geológico Venezolano, Caracas, vol. 10. Sociedad Venezolana de Geólogos, Caracas, pp. 6575–6614.

Bell, J., 1972. Geotectonic evolution of the southern Caribbean area. Geological Society of America Memoir 132, 369–386.

Bellizzia, A., Pimentel, N. and Bajo, R. (compilers), 1976. Mapa geológico-estructural de Venezuela. scale 1:500,000. Ministerio de Minas e Hidrocarburos, Ed. Foninves, Caracas.

Beltrán, C., 1993. Mapa Neotectónico de Venezuela. Scale 1:2,000,000. Funvisis.

Beltrán, C., 1994. Trazas activas y síntesis neotectónica de Venezuela a escala 1:2.000.000. VII Congreso Venezolano de Geofísica, Caracas. Sociedad Venezolana de Ingenieros Geofísicos, Caracas, pp. 541–547.

Beltrán, C., Giraldo, C., 1989. Aspectos neotectónicos de la región nororiental de Venezuela. VII Congreso Geológico Venezolano, Barquisimeto, vol. 3. Sociedad Venezolana de Geólogos, Caracas, pp. 1000–1021.

Benítez, S., 1986. Síntesis geológica del graben de Jambeli. IV Congreso Ecuatoriano de Geología, Minería y Petróleo, vol. 1, 137–160.

Blin, B., 1989. Le front de la chaîne caraïbe vénézuélienne entre la serranía de Portuguesa et la région de Tiznados (surface et subsurface). PhD Thesis, Université de Bretagne Occidentale, Brest, France, 359 pp.

Boinet, T., 1985. La frontière méridionale de la plaque caraïbe aux confins colombo-vénézuéliens (Norte de Santander, Colombie): données géologiques. PhD Thesis, Université de Paris VI, Paris, France, 204 pp + appendices.

Boinet, T., Bourgois, J., Mendoza, H., Vargas, R., 1985. Le poinçon de Pamplona (Colombie): un jalon de la frontière méridionale de la plaque caraïbe. Bulletin de la Societe Geologique de France 8 (I(3)), 403–413.

Bonini, W, Pimstein de Gaete, E. and Graterol, V. (compilers), 1977. Mapa de anomalías de Bouguer de la parte norte de Venezuela y áreas vecinas. Scale 1:1,000,000.M.E.M, Caracas, Venezuela.

Bucher, W., 1952. Structure and orogenic history of Venezuela. Memoir of the Geological Society of America 49, 1–113.

Casas, A., 1991. Estudio sismotectónico del valle del Yaracuy. Funvisis-Universidad de Zaragoza unpublished report.

Case, J.E., Durán, L., López, A., Moore, W., 1971. Tectonic investigations in western Colombia and eastern Panamá. Bulletin of the Geological Society of America 82, 2685–2712.

Castrillo, J., 1997. Structuration néogène du flanc nord-ouest des Andes vénézuéliennes entre Torondoy et Valera. PhD thesis, Université de Pau et des Pays de l'Adour, 247 pp + appendix.

Chalbaud, D., 2000. Determinación del espesor cortical del Escudo

de Guayana a partir del análisis de información de sísmica de refracción. Undergraduate Thesis, Universidad Simón Bolivar, Caracas, 120 pp.

Chalbaud, D., Schmitz, M., Castillo, J., 2000. Determinación del espesor cortical del Escudo de Guayana a través del análisis de información de sísmica de refracción. X Congreso Venezolano de Geofísica. Sociedad Venezolana de Ingenieros Geofísicos, Caracas, 8 pp. (CD-Rom format).

Choy, J., 1998. Profundidad y mecanismo focal del terremoto de El Tocuyo, 1950. Revista Geográfica Venezolana, Instituto de Geografía y Conservación de Recursos Naturales, vol. 39. Universidad de los Andes, Mérida, Venezuela, pp. 203–217.

Cluff, L., Hansen, W., 1969. Seismicity and Seismic Geology of Northwestern Venezuela. Woodward-Clyde and Associates' unpublished report for Shell de Venezuela. Vols. I and II.

Colletta, B., Roure, F., De Toni, B., Loureiro, D., Passalacqua, H., Gou, Y., 1996. Tectonic inheritance and structural styles in the Merida Andes (western Venezuela). 3rd International Symposium on Andean Geodynamics, Saint-Malo, France. Orstom éditions, Paris, pp. 323–326.

Colletta, B., Roure, F., De Toni, B., Loureiro, D., Passalacqua, H., Gou, Y., 1997. Tectonic inheritance, crustal architecture, and contrasting structural styles in the Venezuelan Andes. Tectonics 16 (5), 777–794.

De Cizancourt, H., 1933. Tectonic structure of Northern Andes in Colombia and Venezuela. Bulletin of the American Association of Petroleum Geologists 17 (3), 211–228.

De Toni, B., Kellogg, J., 1993. Seismic evidence for blind thrusting of the northwestern flank of the Venezuelan Andes. Tectonics 12 (6), 1393–1409.

Dewey, J., 1972. Seismicity and tectonics of western Venezuela. Bulletin of the Seismological Society of America 62 (6), 1711–1751.

Duerto, L., 1998. Principales zonas triangulares del Occidente de Venezuela. MSc Thesis, Escuela de Geología, Minas y Geofísica, Universidad Central de Venezuela, 176 pp.

Duerto, L., Audemard, F.E., Lugo, J., Ostos, M., 1998. Síntesis de las principales zonas triangulares en los frentes de montaña del occidente venezolano. IX Congreso Venezolano de Geofísica (in CD-Rom; paper #25).

Duque-Caro, H., 1978. Major structural elements of northern Colombia. Memoir of the American Association of Petroleum Geologists 29, 329–351.

Ego, F., Sébrier, M., Lavenu, A., Yepes, H., Egues, A., 1996. Quaternary state of stress in the Northern Andes and the restraining bend model for the Ecuadorian Andes. Tectonophysics 259 (1–3), 101–116.

Ferrer, C., 1991. Características geomorfológicas y neotectónicas de un segmento de la falla de Boconó entre la ciudad de Mérida y la Laguna de Mucubají, Estado Mérida. Guia de la excursión. Escuela Latinoamericana de Geofísica. Universidad de los Andes, Mérida, Venezuela, 25 pp.

Freymueller, J.T., Kellogg, J.N., Vega, V., 1993. Plate motions in the north Andean region. Journal of Geophysical Research 98, 21853–21863.

Funvisis, 1997. Estudio neotectónico y geología de fallas activas en el piedemonte surandino de los Andes venezolanos (Proyecto INTEVEP 95-061). Funvisis' unpublished report for INTEVEP. 155 pp + appendices.

Giegengack, R., 1984. Late Cenozoic tectonic environments of the central Venezuelan Andes. Geological Society of America Memoir 162, 343–364.

Giraldo, C., 1985. Neotectónica y sismotectónica de la región de El Tocuyo-San Felipe (Venezuela centro-occidental). VI Congreso Geológico Venezolano, Caracas, vol. 4. Sociedad Venezolana de Geólogos, Caracas, pp. 2415–2451.

Giraldo, C., 1989. Valor del desplazamiento dextral acumulado a lo largo de la falla de Boconó, Andes venezolanos. Geos 29, 186–194.

González de Juana, C., 1952. Introducción al estudio de la geología de Venezuela. Boletin de Geologia (Caracas) 2, 407–416.

Grases, J., 1990. Terremotos destructores del Caribe 1502–1990. Orcyt (UNESCO), Montevideo, Uruguay, 132 pp.

Henneberg, H., 1983. Geodetic control of neotectonics in Venezuela. Tectonophysics 97, 1–15.

Hospers, J., Van Wijnen, J., 1959. The gravity field of the Venezuelan Andes and adjacent basins. Verslag van de Gewone Vergadering van de Afdeling Natuurkunde, Koninklijke Nederlandse Akademie van Wetenschappen 23 (1), 1–95.

Jácome, M., 1994. Interpretación geológica, sísmica y gravimétrica de un perfil transandino. Undergraduate Thesis, Universidad Simón Bolívar, Caracas, Venezuela, 68 pp.

Jácome, M., Audemard, F.E., Graterol, V., 1995. A seismic, gravimetric and geologic interpretation of a transandean profile across the Venezuelan Andes. I Latinoamerican Geophysical Congress, Rio de Janeiro, Brazil, pp. 15–18.

Jordan, T., 1975. The present-day motions of the Caribbean plate. Journal of Geophysical Research 80, 4433–4439.

Kaniuth, K., Drewes, H., Stuber, K., Temel, H., Hernández, J.N., Hoyer, M., Wildermann, E., Kahle, H., Geiger, G., 1999. Position changes due to recent crustal deformations along the Caribbean–South American plate boundary derived from CASA GPS project. General Assembly of the International Union of Geodesy and Geophysics (IUGG), Birmingham, U.K. Poster at Symposium G1 of International Association of Geodesy.

Kellogg, J., Bonini, W., 1982. Subduction of the Caribbean plate and basement uplifts in the overriding south-American plate. Tectonics 1 (3), 251–276.

Kellogg, J., Vega, V., 1995. Tectonic development of Panama, Costa Rica, and the Colombian Andes: constraints from global positioning system geodetic studies and gravity. Special Paper-Geological Society of America 295, 75–90.

Kohn, B., Shagam, R., Banks, P., Burkley, L., 1984. Mesozoic–Pleistocene fission track ages on rocks of the Venezuelan Andes and their tectonic implications. Geological Society of America Memoir 162, 365–384.

Malavé, G., Suárez, G., 1995. Intermediate-depth seismicity in northern Colombia and western Venezuela and its relationship to Caribbean plate subduction. Tectonics 14 (3), 617–628.

Malfait, B., Dinkelman, M., 1972. Circum-Caribbean tectonic and igneous activity and the evolution of the Caribbean plate. Geological Society of America Bulletin 83 (2), 251–272.

Mattauer, M., 1983. Subduction de lithosphère continentale, décollement croûte-manteau et chevauchement d'échelle crustale

dans la chaîne de collision himalayenne. Comptes Rendus de l'Academie des Sciences, Paris 296, 481–486.

Mattauer, M., 1985. Intracontinental subduction, crust-mantle decollement and crustal stacking wedge in the Himalaya and other collision belts. Collision Tectonics, Geological Society Special Publication, vol. 14. Geological Society of London, pp. 363–385.

Mattauer, M., Matte, P., Olivet, J.-L., 1999. A 3D model of the India–Asia collision at plate scale. Compte Rendus de l'Academie des Sciences, Paris 328, 499–508.

McCann, W., Pennington, W., 1990. Seismicity, large earthquakes, and the margin of the Caribbean plate. In: Dengo, D., Case, J.E. (Eds.), The Caribbean region. The Geology of North America, v. H.. Geological Society of America, Boulder, USA, pp. 291–306.

Minster, J., Jordan, T., 1978. Present-day plate motions. Journal of Geophysical Research 83, 5331–5354.

Molnar, P., Sykes, L., 1969. Tectonics of the Caribbean and middle America regions from focal mechanisms and seismicity. Geological Society of America Bulletin 80, 1639–1684.

Padrón, C., Izarra, C., 1996. Modelo de velocidad 1D para el occidente de Venezuela. VIII Congreso Venezolano de Geofísica, Maracaibo. Sociedad Venezolana de Ingenieros Geofísicos, Caracas, pp. 401–408.

Peltzer, G., Tapponnier, P., 1988. Formation and evolution of strike-slip faults, rifts and basins during the India–Asia collision: an experimental approach. Journal of Geophysical Research 93, 15085–15117.

Pennington, W., 1981. Subduction of the eastern Panama basin and seismotectonics of northwestern south America. Journal of Geophysical Research 86 (B11), 10753–10770.

Pérez, O., Jaimes, M., Garciacaro, E., 1997. Microseismicity evidence for subduction of the Caribbean plate beneath the south American plate in northwestern Venezuela. Journal of Geophysical Research 102 (B8), 17875–17882.

Pérez, O., Aggarwal, Y., 1981. Present-day tectonics of southeastern Caribbean and northeastern Venezuela. Journal of Geophysical Research 86, 10791–10805.

Pindell, J., Dewey, J., 1982. Permo-Triassic reconstruction of western Pangea and the evolution of the Gulf of Mexico/Caribbean region. Tectonics 1 (2), 179–211.

Pindell, J., Cande, S., Pitman III, W., Rowley, D., Dewey, J., LaBrecque, J., Haxby, W. 1988. A plate-kinematic framework for models of Caribbean evolution. Tectonophysics 155, 121–138.

Rod, E., 1956a. Earthquakes of Venezuela related to strike slip faults? American Association of Petroleum Geologists Bulletin 40, 2509–2512.

Rod, E., 1956b. Strike-slip faults of northern Venezuela. American Association of Petroleum Geologists Bulletin 40, 457–476.

Rod, E., 1960. Comments on "The gravity field of the Venezuelan Andes and adjacent basins". Boletin Informativo Asociacion Venezolana de Geologia, Mineria y Petroleo 3, 170–175.

Rod, E., Jefferson, C., Von Der Osten, E., Mullen, R., Graves, G., 1958. The determination of the Bocono fault. Boletin Informativo Asociacion Venezolana de Geologia, Mineria y Petroleo 1 (1–6), 69–100.

Ross, M., Scotese, C., 1988. A hierarchical tectonic model of the Gulf of Mexico and Caribbean region. Tectonophysics 155, 139–168.

Sánchez, M., Audemard, F.E., Giraldo, C., Ruiz, F., 1994. Interpretación sísmica y gravimétrica de un perfil a través de los Andes venezolanos. Memorias VII Congreso Venezolano de Geofísica, Caracas. Sociedad Venezolana de Ingenieros Geofísicos, Caracas, pp. 251–258.

Schmitz, M., Chalbaud, D., Castillo, J., Izarra, C., Lüth, S., 1999. The crustal structure and isostatic balance of the Guayana Shield, Venezuela. 4th International Symposium on Andean Geodynamics, Göttingen, Germany. Institut de Recherche pour le Développement–IRD, Paris, pp. 663–667 (extended abstract).

Schubert, C., 1968. Geología de la región de Barinitas–Santo Domingo. Andes Venezolanos Surorientales. Boletin de Geologia (Caracas) 10, 161–181.

Schubert, C., 1980a. Morfología neotectónica de una falla rumbo-deslizante e informe preliminar sobre la falla de Boconó, Andes merideños. Acta Cientifica Venezolana 31, 98–111.

Schubert, C., 1980b. Late Cenozoic pull-apart basins, Boconó fault zone, Venezuelan Andes. Journal of Structural Geology 2 (4), 463–468.

Schubert, C., 1982. Neotectonics of the Boconó fault, western Venezuela. Tectonophysics 85, 205–220.

Schubert, C., 1984. Basin formation along Boconó-Morón-El Pilar fault system, Venezuela. Journal of Geophysical Research 89, 5711–5718.

Schubert, C., 1985. Comments on "Subduction of the Caribbean Plate and Basement Uplifts in the overriding South-American Plate" by J.N. Kellogg, and W.E. Bonini. Tectonics 4 (7), 781–783.

Shagam, R., Kohn, B., Banks, P., Dasch, L., Vargas, R., Rodríguez, G., Pimentel, N., 1984. Tectonic implications of cretaceous–pliocene fission track ages from rocks of the circum-Maracaibo Basin region of western Venezuela and eastern Colombia. Geological Society of America Memoir 162, 385–412.

Shemenda, A., 1993. Subduction of lithosphere and back-arc dynamics: insights from physical modeling. Journal of Geophysical Research 98, 16167–16185.

Singer, A., Audemard, F.A., 1997. Aportes de Funvisis al desarrollo de la geología de fallas activas y de la paleosismología para los estudios de amenaza y riesgo sísmico. In: Grases, J. (Ed.), Diseño sismorresistente. Especificaciones y criterios empleados en Venezuela. Publicación Especial, vol. 33. Academia de las Ciencias Naturales, Matemáticas y Físicas, Caracas, pp. 25–38.

Singer, A., Beltrán, C., 1996. Active faulting in the Southern Venezuelan Andes and Colombian borderland. 3rd International Symposium on Andean Geodynamics, Saint-Malo, France. Orstom éditions, Paris, pp. 243–246.

Soulas, J.-P., 1985. Neotectónica del flanco occidental de los Andes de Venezuela entre 70°30′ y 71°00′ W (Fallas de Boconó, Valera, Piñango y del Piedemonte). VI Congreso Geológico Venezolano, Caracas, vol. 4. Sociedad Venezolana de Geólogos, Caracas, pp. 2690–2711.

Soulas, J.-P., 1986. Neotectónica y tectónica activa en Venezuela y regiones vecinas. VI Congreso Geológico Venezolano, Caracas-1985, vol. 10. Sociedad Venezolana de Geólogos, Caracas, pp. 6639–6656.

Soulas, J.-P. and Singer, A., 1987. Mapa "Evidencias de actividad cuaternaria en las fallas". In: Soulas, J.-P., Singer, A. and Lugo, M., 1987. Tectónica cuaternaria, características sismogénicas de las fallas de Boconó, San Simón y del piedemonte occidental andino y efectos geológicos asociados a la sismicidad histórica (Proyecto Sumandes). Funvisis' unpublished report for Maraven S.A., 90 pp.

Soulas, J.-P., Rojas, C., Schubert, C., 1986. Neotectónica de las fallas de Boconó, Valera, Tuñame y Mene Grande: Excursión No. 4. VI Congreso Geológico Venezolano, Caracas-1985, vol. 10. Sociedad Venezolana de Geólogos, Caracas, pp. 6961–6999.

Stephan, J.-F., 1982. Evolution géodinamique du domaine Caraïbe, Andes et chaîne Caraibe sur la transversale de Barquisimeto (Vénézuéla). PhD Thesis, Paris, 512 pp.

Stephan, J.-F., 1985. Andes et chaîne Caraïbe sur la transversale de Barquisimeto (Vénézuéla). Evolution géodinamique. Symposium Géodynamique des Caraïbes, Paris. éditions Technip, Paris, pp. 505–529.

Stephan, J.-F., Mercier De Lepinay, B., Calais, E., Tardy, M., Beck, C., Carfantan, J.-C., Olivet, J.-L., Vila, J.-M., Bouysse, P., Mauffret, A., Bourgois, J., Thery, J.-M., Tournon, J., Blanchet, R., Dercourt, J., 1990. Paleogeodynamic maps of the Caribbean: 14 steps from Lias to Present. Bulletin de la Societe Geologique de France 6 (6), 915–919.

Suárez, G., Nábelek, J., 1990. The 1967 Caracas earthquake: fault geometry, direction of rupture propagation and seismotectonic implications. Journal of Geophysical Research 95 (B11), 17459–17474.

Sykes, L., McCann, W., Kafka, A., 1982. Motion of Caribbean Plate during last 7 million years and implications for earlier Cenozoic movements. Journal of Geophysical Research 87 (B13), 10656–10676.

Taboada, A., Rivera, L.A., Fuenzalida, A., Cisternas, A., Philip, H., Bijwaard, H., Olaya, J., Rivera, C., 2000. Geodynamic of the northern Andes: subductions and intracontinental deformation (Colombia). Tectonics 19 (5), 787–813.

Tapponnier, P., Molnar, P., 1976. Slip-line field theory and large-scale continental tectonics. Nature 264, 319–324.

Van der Hilst, R., 1990. Tomography with P, PP and pP delay-time data and the three dimensional mantle structure below the Caribbean region. Geologica Ultraiectina, vol. 67. University of Utrecht, Netherlands, 250 pp.

Van der Hilst, R., Mann, P., 1993. Tectonic implication of tomographic images of subducted lithosphere beneath northwestern South America. AAPG/SVG International Congress and Exhibition. American Association of Petroleum Geologists/Sociedad Venezolana de Geólogos, Caracas, p. 71, abstract.

Wadge, G., Burke, K., 1983. Neogene Caribbean plate rotation and associated central American tectonic evolution. Tectonics 2 (6), 633–643.